Structural Flexibility of a Copper-Based Metal Organic Framework: Adsorption of C_4-hydrocarbons and *in situ* XRD

Journal:	*Journal of Materials Chemistry A*
Manuscript ID:	TA-ART-12-2013-015331.R1
Article Type:	Paper
Date Submitted by the Author:	25-Feb-2014
Complete List of Authors:	Lange, Marcus; Institut für Nichtklassische Chemie e.V. an der Universität Leipzig, Kobalz, Merten; Universität Leipzig, Institut für Anorganische Chemie Bergmann, Jens; Universität Leipzig, Institut für Anorganische Chemie Lässig, Daniel; Universität Leipzig, Institut für Anorganische Chemie Lincke, Jörg; Universität Leipzig, Institut für Anorganische Chemie Möllmer, Jens; Universität Leipzig, Institut f. Nichtklassische Chemie e.V. Moeller, Andreas; INC, Hofmann, Jörg; Institut für Nichtklassische Chemie e.V. an der Universität Leipzig, Krautscheid, Harald; Universitaet Leipzig, Anorganische Chemie Staudt, Reiner; Hochschule Offenburg, Fakultät Maschinenbau und Verfahrenstechnik Gläser, Roger; INC,

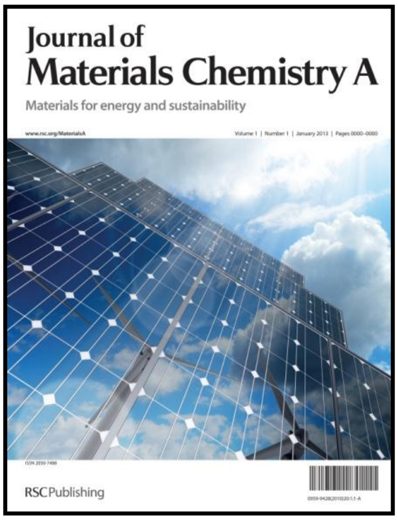

Journal of Materials Chemistry A

Materials for Energy and Sustainability

Full paper submission

Journal of Materials Chemistry A is a weekly journal in the materials field. The journal is interdisciplinary, publishing work of international significance on all aspects of materials chemistry related to energy and sustainability. Articles cover the fabrication, properties and applications of materials.

2012 Impact Factor of *Journal of Materials Chemistry*: **6.10**
For more information go to www.rsc.org/materialsA

The following paper has been submitted to *Journal of Materials Chemistry A* for consideration as a **full paper**.

Journal of Materials Chemistry A wishes to publish original research that demonstrates **novelty and advance**, either in the chemistry used to produce materials or in the properties/applications of the materials produced. Work submitted that is outside of these criteria will not usually be considered for publication. The materials should also be related to the theme of materials for energy and sustainability.

Routine or incremental work, however competently researched and reported, should not be recommended for publication if it does not meet our expectations with regard to novelty and impact.

It is the responsibility of authors to provide fully convincing evidence for the homogeneity and identity of all compounds they claim as new. Evidence of both purity and identity is required to establish that the properties and constants reported are those of the compound with the new structure claimed.

Thank you for your effort in reviewing this submission. It is only through the continued service of referees that we can maintain both the high quality of the publication and the rapid response times to authors. We would greatly appreciate if you could review this paper in **two weeks**. Please let us know if that will not be possible.

Once again, we appreciate your time in serving as a reviewer. To acknowledge this, the RSC offers a **25% discount** on its books: http://www.rsc.org/Shop/books/discounts.asp. Please also consider submitting your next manuscript to *Journal of Materials Chemistry A*.

Best wishes,

Liz Dunn

Liz Dunn
Managing Editor, *Journal of Materials Chemistry A*

Structural Flexibility of a Copper-Based Metal Organic Framework: Adsorption of C_4-hydrocarbons and *in situ* XRD

Marcus Lange,[a] Merten Kobalz,[b] Jens Bergmann,[b] Daniel Lässig,[b] Jörg Lincke,[b] Jens Möllmer,[a] Andreas Möller,[a] Jörg Hofmann,[a] Harald Krautscheid,[b] Reiner Staudt[c] and Roger Gläser*[a]

Manuscript ID TA-ART-12-2013-015331

List of changes made during revision of the manuscript

Changes are marked in yellow in the revised manuscript.

In response to the reviewers' comments:

First of all, we would like to thank the reviewers for their helpful comments and detailed criticism. In the following, we will respond to the individual comments.

In response to reviewer 1:

1. **Comment:** The adsorption curve of 1-butene shows at 283K a second broad hysteresis at a pressure of 100kPa (P/P0= 0.67). In the case of the adsorption of butane, only one hysteresis is present. If we consider that these two C4-hydrocarbons have a similar "effective" size, I don't understand why the butane isotherm doesn't show a second hysteresis. It seems reasonable to think that we should have similar uptake with these two molecules. Because the isotherms are built using absolute pressure, is it possible that 100 kPa is not enough high in the case of butane to induce this second gate opening. In other words, what is the behavior of the butane isotherm at higher pressure? Does the authors have performed in situ XRD at higher pressure?

   Response: The reviewer is right in assuming an additional gate opening at higher pressures of n-butane in view of the quite similar molecular characteristics, in particular effective molecular dimensions. This was the reason for conducting sorption experiments close to relative pressure p/p0 = 1. In Fig. SI 5, the isotherms of the investigated C4-isomers are plotted versus relative pressure at 283 K in logarithmic scale. Certainly, a pressure of 100 kPa is evidently too low to induce a second transformation. The second broad hysteresis for 1-butene sorption starts at p/p0 = 0.54. Although n-butane isotherm is shown only up to a relative pressure of p/p0 = 0.68, the isotherms does not show any further hysteresis. However, at higher n-butane pressures, we observed a loading increase as a result of condensation between the (macroscopic) particles. This observation was confirmed by desorption that offers the same loadings as found for adsorption and not a hysteresis as would be expected for an additional gate opening. The authors added

Fig. SI 6, displaying isotherms versus relative pressure in a linear scale to elucidate the second transformation range.

In addition, the sorption isotherm of 1-butene taken at 298 K up to 253 kPa (p/p0 = 0.84) shows a second broad hysteresis loop opening at a pressure of 187 kPa (p/p0 = 0.62). The n-butane isotherm was measured up to 221 kPa corresponding to a higher relative pressure of p/p0 = 0.91 due to the lower saturation vapor pressure. Sorption of n-butane does not offer a second transformation even though compared to 1-butene sorption at 298 K a higher relative pressure was achieved.

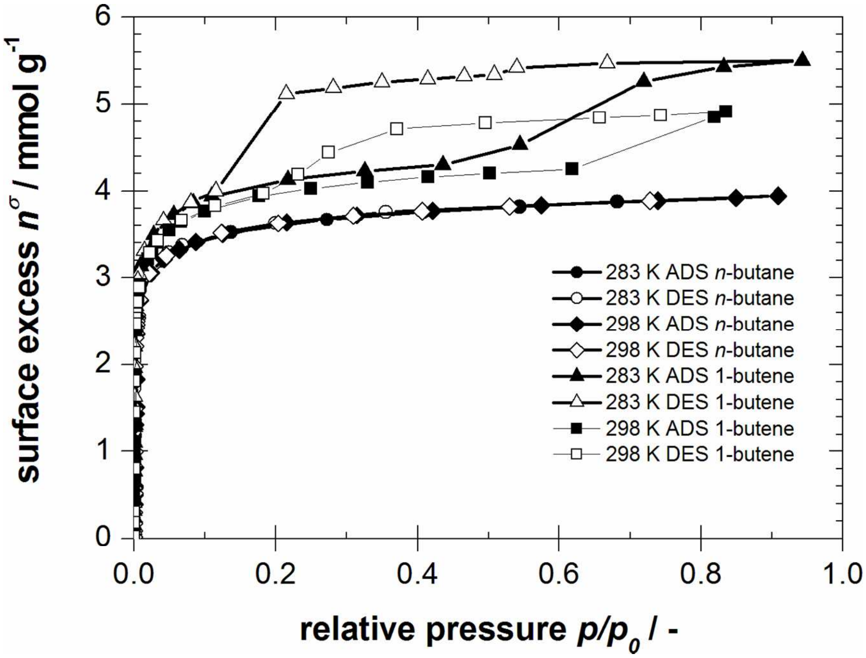

Moreover, the in situ XRD experiments were performed up to 265 kPa at room temperature resulting in relative pressures close to p/p0 = 1. The resulting XRD-patterns of investigated C4-isomers at these pressures are compared in Fig. SI 9. The pattern of 1-butene at 209 kPa is similar to those of n-butane, isobutane and isobutene at 265 kPa, respectively. However, at higher pressures, only the pattern of 1-butene shows an additional structural transformation.

2. **Comment:** The authors should be careful with the interpretation of the behavior of the Qst. Indeed, if we look at the adsorption curve of butane and isobutene, both of them show a hysteresis attributed to a gate opening phenomena; but the behavior of the associated Qst in the range of coverage from 0 to 0.6 is totally different. The gate opening also provides new sites during the adsorption process of butane that should also involve an increase of Qst following the explanation gave by the authors. But, it’s not the case. Accordingly, the origin of evolution of the Qst is certainly due to a combination of different phenomena including the gate opening.

   Action taken: We want to thank the reviewer for this helpful comment. Indeed, the curve shape of isosteric heat is hard to interpret with gate opening. As mentioned by the reviewer, structural transformation may provide new sorption sites which could lead to an increase in the heat of adsorption. It is also right that gate opening is a process including several phenomena, e.g., an exothermic structural transition, and we only observe the superposition of these effects. We also have to consider that adsorption enthalpies only were calculated (and not experimentally assessed directly, e.g., by caloric techniques). Nevertheless, the model is approved and widely used in the literature.

Accordingly, the paragraph dealing with heat of adsorption (page 6, line 21 – 51) was modified as follows:

From Fig. 6 it becomes obvious, that the isosteric heat of adsorption on **1** is in a close region between 40 and 50 kJ mol^{-1} for all adsorptives at zero coverage and expectedly decreases with higher coverage. The heat of adsorption of *n*-butane on **1** is the highest for coverage up to $\Theta = 0.8$. Regarding low coverages until $\Theta = 0.2$, the lowest value is observed for isobutene. However, between $\Theta = 0.2$ and $\Theta = 0.6$ it just decreases slightly for all sorptives assuming a dependence on the gate opening process which generates new sorption sites. A peculiarity is observed for isobutane, where a sharp minimum in the isosteric heat of adsorption is observed at a coverage of $\Theta = 0.2$. This is a result of the reached well-defined plateau in the sorption isotherm indicating a nearly complete pore filling of **1**, before the first crystal-to-crystal transformation occurs (cf. Fig 2). This results in the striking drop in the heat of adsorption at coverage of $\Theta = 0.2$ due to reduced interaction between sorptive and adsorbent surface. While the gate opening proceeds, new adsorption sites are generated and occupied by adsorptive molecules resulting in an increase of the isosteric heat of adsorption. For the other sorptives this effect is indistinct because the isotherms do not show such a defined saturation plateau for first pore filling followed by a sharp rise of loading. Here, energetically equal sorption sites are available during the whole sorption process until the first structural transformation occurs. For 1-butene adsorption, a second gate opening at higher pressures was observed in the isotherm, which again leads to an increase of the isosteric heat of adsorption at higher coverage ($\theta = 0.8$).

In response to reviewer 2:

1. **Comment:** The adsorption enthalpy is higher for the paraffin compared to the corresponding olefin. This someone unusual finding should be discussed based on the MOF structure. What are the prime adsorption sites.

   Response: The reviewer is right that it is quite unusual for paraffins to exhibit higher heat of adsorption than olefins, which was also surprising for us. However, there is no doubt regarding the validity of our experimental data. Indeed, the adsorption enthalpy is related to the interaction of sorptive and adsorbent, i.e. MOF surface. Unfortunately, the current study does allow to identify the “prime adsorption sites”. It is conceivable that, especially at higher loadings, i.e., after gate opening, 1-butene interacts with the five-coordinated copper-ions. This could lead to a second structural change. Since, however, we do not have direct experimental proof for this assumption, we chose not to make prominent statements on the adsorption sites.

2. **Comment:** The structural changes associated with the gate opening remain unclear. I do understand that structure determination is difficult from powder data, but some suggestions would be beneficial for the reader.

   Action taken: From the reversibility of the gate opening process, we know that the connectivity of the framework is not changed. Hence, the origin of the flexibility has to be located in the linker molecules, in particular the dihedral angle between triazolyl- and phenyl ring. Moreover, the tolerance of the angle between the [Cu4(μ4-O)(μ2-OH)2]4+-SBU and the coordinating triazolyl- and carboxylic group is beneficial for structural transitions. After activation, **1** offers sufficient crystallinity for qualitative observation of changes in the diffraction pattern originating in structural changes. However, due to reduced crystallinity, the quality of the diffraction pattern is not good enough for structure solution: There are not enough reflections and moreover theses are too broad.

   What we can extract from our data, is disappearing and new formation of reflections. This indicates a structural change. Nevertheless, we are not yet able to discuss structural details in this paper.

   The authors modified the first two paragraphs in 3.3 In situ XRD studies (page 7, line 11 – 64):

   After activation, i.e. the removal of guest molecules, **1** shows sufficient crystallinity for qualitative observation of changes in the X-ray diffraction pattern. However, due to reduced crystallinity, the quality of the diffraction pattern is not good enough for structure solution. Hence, it was possible to monitor structural changes by means of changes in the ~~X-ray~~ diffraction pattern during C_4-hydrocarbon sorption on **1** at room temperature up to saturated vapor pressures. Fig. 7 presents the pressure dependent X-ray diffraction patterns of **1** at different loadings with 1-butene. A small aperture for 2θ between 6 ° and 12 ° is chosen because the material shows the strongest reflections in this range (cf. Fig. SI 8). Hence, changes in the diffraction pattern due to structural changes can be pointed out most sensitively in this region. At certain pressures, powder patterns were recorded corresponding to different C_4-hydrocarbon loadings.

   From the diffraction patterns it can be concluded that for low loadings the structure is similar to that of the evacuated material (cf. Fig 7, points 1 and 2). Thus, there are two strong reflections (2θ = 7.5 ° and 8.7 °) and a weak one (9.4 °). With increasing 1-butene pressure, the pattern changes according to a structural change starting at 1.2 kPa (point 3). Disappearing and new formation of reflections indicates a structural change.

   There might be a coexistence of two structures over a certain pressure range (points 3 and 4). At a pressure of about 75 kPa, the newly formed phase is present (points 5 and 6). Whereas the reflection at 7.5 ° disappears during adsorption, a new reflection appears at 7.7 °. In addition the peak at 8.7 ° is shifted with increasing pressure to 8.5 ° (points 1-3) and disappears at 10.33 kPa (point 4). In contrast, beginning at 1.20 kPa a new reflection is observed at 8.8 ° which is also shifted to lower diffraction angles (points 3-7). Since the diffraction patterns of point 1 (0.25 kPa) and point 5 (76.45 kPa) are completely unrelated, structural changes, corresponding to a gate opening process, are clearly evident. In particular, the pattern at point 3 shows reflections of both phases of point 2 and point 4. Thus the coexistence of particles/domains of the evacuated phase and the phase after the first gate opening is proved. For 1-butene, a second gate opening is observed above 210 kPa. In the associated pattern at 290 kPa (point 7), an additional peak appears at 7.2 °. This pattern resembles that of the solvated material obtained after Soxhlet extraction of the as-synthesized MOF material **1** with methanol (cf. Fig. SI 9). This indicates that 1-butene is able to induce structural transformations and reformation of the structure of the as-synthesized material indicated by powder patterns similar to the pristine MOF filled with methanol. As a conclusion, during the adsorption of 1-butene at 283 K the framework of **1** undergoes a crystal-to-crystal reformation according to Kitagawa`s type III category[5,6]. Contrary, the adsorption of isobutene, isobutane and *n*-butane does not cause a complete reformation. As a result, this observation makes it difficult to classify flexible metal-organic frameworks only with respect to their types of adsorption isotherms, in particular, materials like **1** can be assigned to more than one type.

3. **Comment:** Is gate opening possible by temperature changes? Please comment.

   Response: The reviewer probably thinks of the application of flexible MOFs in temperature-swing processes. The authors agree that this would be interesting for further investigations.

   From our studies, we can state that temperature change under constant pressure should also offer gate opening/closing phenomena. In Fig. 5, the temperature-dependence of gate opening pressure is presented. With a closer view to the isotherms, it appears feasible that a gate opening occurs in dependence of temperature. For n-butane sorption on **1** for example, a pressure of 1 kPa leads to n-butane adsorption of 2.86 mmol g-1 at 283 K. By increasing the temperature to 343 K at constant pressure, the loading decreases drastically (and clearly more than expected merely for a temperature increase) to 0.57 mmol g-1 indicating gate closing and vice versa. Moreover, there are several contributions of temperature-dependent gate opening/closing phenomena observed for other MOFs such as IM-19 [G. Chaplais, A. Simon-Masseron, F. Porcher, C. Lecomte, D. Bazin-Bachi, N. Bats, J. Patarin, *Phys. Chem. Chem. Phys.*, 2009, 11, 5241–5245], [Zn2(fu-L)2dabco]n [S. Henke, A. Schneemann, R. A. Fischer, *Adv. Funct. Mater.*, 2013, **23**, 5990–5996] and MIL-53/-47 [T. K. Trung, I. Deroche, A. Rivera, Q. Yang, P. Yot, N. Ramsahye, S. D.Vinot, T. Devic, P. Horcajada, C. Serre, G. Maurin, P. Trens, *J. Mater. Chem.*, 2011, **21**, 3070-3076, Y.Liu, J.-H.Her, A.Dailly, A.J.Ramirez-Cuesta, D.A.Neumann, C.M.Brown, *J. Am. Chem. Soc.*, 2008, **130**, 11813–11818]. Since this manuscript is focused on the pressure dependence (rather than the temperature dependence) in relation to the structural changes, we decided not to include a discussion on the temperature effects on the gate transitions of the MOF materials.

Itemized list of changes

In addition, the authors corrected various typing errors and added some issues.

Page 1, line 4: “Reiner Staudt[c] and Roger Gläser[*a]“ instead of “Roger Gläser[a,b] and Reiner Staudt[c]”

Page 1, line 9: “343 K and pressures“ instead of “343 Kand pressures”

Page 1, line 10: “Gate opening“ instead of „Gateopening“

Page 1, line 55: “most intensely“ instead of „best“

Page 2, line 35: “intention” instead of “intension”

Page 3, line 15: “~~(glass capillary)~~” should be deleted

Page 3, line 61: “pressure,”

Page 4, line 6: “(p/p0 = 0.54) instead of “(p/p0 = 0.67)”

Page 4, line 6-7: “up to 175 kPa (p/p0 = 0.94)” was added

Page 4, line 83: “, studied here,“ instead of „(this study)“

Page 4, line 85: „e.g.,“ instead of „e.g.”

Page 5, line 7: “opening pressure“ instead of „opening pressure“

Page 5, line 10: „e.g.,“ instead of „e.g.”

Page 5, line 12: „ isobutene and isobutane “ instead of „ isobutene and isobutene”

Page 5, line 21: „i.e.,“ instead of „i.e.”

Page 6, line 3, Table 3 Footnotes: „[2]After 2nd transition“ instead of „[1]After 2nd transition”

Page 6, line 29: „ which generates new sorption sites” was added

Page 6, line 32: „ in the sorption isotherm” was added

Page 6, line 36-37: „ due to reduced interaction between sorptive and adsorbent surface” was added

Page 6, line 45-46: „ defined saturation plateau for first pore filling followed by a” was added

Page 6, line 46-48: „ Here, energetically equal sorption sites are available during the whole sorption process until the first structural transformation occurs.” was added

Page 7, line 12-15: „ for qualitative observation of changes in the X-ray diffraction pattern. However, due to reduced crystallinity, the quality of the diffraction pattern is not good enough for structure solution.” was added

Page 5, line 15: „ monitor “ instead of „elucidate”

Page 7, line 16: “~~X-ray~~ ” should be deleted

Page 7, line 22: „ the diffraction pattern” was added

Page 7, line 31-32: „ Disappearing and new formation of reflections indicates a structural change.” was added

Page 7, line 45: “evident“ instead of „evidence“

Page 7, line 45-48: „ In particular, the pattern at point 3 shows reflections of both phases of point 2 and point 4. Thus the coexistence of particles/domains of the evacuated phase and the phase after the first gate opening is proved.” was added

Page 7, line 54-55: „ of the structure of the as-synthesized material” was added

Page 7, line 58: „ crystal-to-crystal” instead of “crystal-to crystal”

Page 7, line 59-61: „ Contrary, the adsorption of isobutene, isobutane and *n*-butane does not cause a complete reformation.” was added

Page 7, line 66: “~~similar~~” should be deleted

Page 8, line 48: “on **1**, its“ instead of „on **1** its”

Page 8, line 57: “Lincke et al.[42]“ instead of„Lincke et al.:”

Page 8, line 58: “methanol, the“ instead of „methanol the”

Page 8, line 63: “study, the“ instead of „study the”

Page 8, line 67: “of the C_4-hydrocarbons” instead of “of C_4-hydrocarbons”

Page 8, line 80: “Gurvich’s rule” instead of “the Gurvich-rule”

Page 8, line 81: “comparable” instead of “similar”

Page 9, line 24-28: „ From that only 1-butene affected a complete crystal-to-crystal reformation of the structure of the as-synthesized material, whereas the adsorption of isobutane, isobutene and *n*-butane only leads to a partial reformation.” was added/changed

Page 9, line 28-30: „ The structural changes are accompanied by disappearance and new formation of reflections in the XRD pattern.” was added

Page 9, line 39-40: “STA 428/17-2 KR 1675/7-2 and GL 290/6-2” instead of “STA 428/17-1 and KR 1675/7-2“

Page 9, line 40-45: „ The University of Leipzig (PbF-1), and the graduate school BuildMoNa are gratefully acknowledged. D.L. acknowledges the fellowship of the Fonds der Chemischen Industrie. J.L. is grateful for an ESF fellowships. This work was funded by the European Union and the Free State of Saxony.” was added/changed

Page 9, line 49: “+49 (0)341 235 2701“ instead of „+49 (0)341 235 2702“

Page 9, line 54: “^{c}“ instead of „^{b}“

Journal of Materials Chemistry A

Dynamic Article Links ►

Cite this: DOI: 10.1039/c0xx00000x

www.rsc.org/xxxxxx

Full Paper

Structural Flexibility of a Copper-Based Metal Organic Framework: Adsorption of C_4-hydrocarbons and *in situ* XRD

Marcus Lange,[a] Merten Kobalz,[b] Jens Bergmann,[b] Daniel Lässig,[b] Jörg Lincke,[b] Jens Möllmer,[a] Andreas Möller,[a] Jörg Hofmann,[a] Harald Krautscheid,[b] Reiner Staudt[c] and Roger Gläser*[a]

Received (in XXX, XXX) Xth XXXXXXXXX 20XX, Accepted Xth XXXXXXXXX 20XX
DOI: 10.1039/b000000x

Pure component sorption isotherms of *n*-butane, isobutane, 1-butene and isobutene on the metal-organic framework (MOF) $^{3}_{\infty}[Cu_4(\mu_4\text{-}O)(\mu_2\text{-}OH)_2(Me_2trz\text{-}pba)_4]$ at various temperatures between 283 K and 343 K and pressures up to 300 kPa are presented. The isotherms show a stepwise pore filling which is typical for structurally flexible materials with broad adsorption/desorption hysteresis loops. Gate opening pressures in their endemic characteristic depend on the used hydrocarbon gases. From all investigated gases only the isotherms of 1-butene present a second step at a relative pressure above $p/p_0 = 0.55$. As a consequence, only 1-butene can fully open the framework resulting in a pore volume of 0.54 $cm^3\ g^{-1}$. This result is in good agreement with the value of 0.59 $cm^3\ g^{-1}$ calculated based on single crystal structure data. The isosteric heat of adsorption was calculated from the experimental isotherms for all C_4-isomers. At low loadings the isosteric heat is in a close region between 41 and 49 kJ mol^{-1}. For all sorption experiments, in particular, only one batch of the MOF material was used without any adverse effect on sorption capacity and framework flexibility meaning that the material was stable. Moreover, *in situ* XRD measurements at different relative hydrocarbon pressures were performed at 298 K for the C_4-isomers. The differences in the pressure-depending powder diffraction patterns indicate phase transitions as a result of adsorption. Similar diffraction patterns were observed for all C_4-hydrocarbons, except 1-butene, where the second step at higher relative pressure ($p/p_0 > 0.55$) is accompanied by an additional phase transition. This powder pattern resembles that of the as-synthesized MOF material containing solvent molecules in the pore system. The resulting structural changes of the material during guest and pressure induced external stimuli are evidenced by the newly coupled XRD adsorption equipment.

1. Introduction

Since the development of metal-organic frameworks (MOFs)[1-4] or porous coordination polymers (PCPs)[5,6] in the last one and a half decades, this class of materials has gained increasing interest in research. The enormous variability of these materials due to different linkers and metal ions or secondary building units (SBUs) allows several applications, e.g., in sensor devices[7-9], in heterogeneous catalysis[10-14] as well as for gas storage[15-19] or gas separation[20-26].

One of the basic requirements for using such materials in sorption processes is the complete removal of pre-adsorbed solvent molecules and residues remaining from synthesis by pretreatment, i.e. evacuation with or without heating. Regarding their different behavior during the activation procedure Kitagawa et al.[5,6] suggested a classification resulting in three different generations of materials. Within the third generation three types of flexible MOFs can be distinguished[6]: type I – "recoverable collapsing" MOFs, type II – "guest-induced transformation" frameworks and type III – "guest-induced reformation" MOFs. Referring to type II and type III materials, different sorption isotherm curvatures are noticeable due to the structural flexibility. There are flexible MOFs which seem to be non-porous after activation, while others show a porous character which leads, in particular, to a stepwise adsorption-desorption isotherm. Such isotherms reveal a so called *gate opening pressure* at which the framework undergoes a structural change along with a sudden increase in adsorption capacity.[6,27] The phenomenon of structural flexibility are results of several different external stimuli like temperature, pressure or light.[6,27-36,]

Two of the most intensely studied flexible MOFs are MIL-53-Cr[32] and MIL-53-Al.[33] Serre et al.[32-37] were able to elucidate the structural changes of MIL-53(Cr) through pressure- or temperature-dependent X-ray powder diffraction (XRD). After activation this material shows a large pore phase (lp). During adsorption of water or CO_2 a structural change to a narrow pore phase (np) is observed. This is caused by the strong interaction of the guest molecules with the framework. By increasing the CO_2-pressure the network expands to give the lp form. The reversibility of this so-called breathing effect was shown by pressure dependent X-ray powder diffraction.[35]

Recently, we presented the synthesis, crystal structure and adsorption data on the new flexible Cu-based MOF $^{3}_{\infty}[Cu_4(\mu_4\text{-}O)(\mu_2\text{-}OH)_2(Me_2trz\text{-}pba)_4]$ (**1**)[42;43]. With several sorptives including CO_2, N_2, Ar, CH_4 or MeOH, the isotherms revealed a stepwise pore-filling with one or two hysteresis loops and different gate opening pressures for each sorptive and temperature[42]. In particular, sorption isotherms of subcritical gases like CO_2 (298 K and 273 K), CH_3OH (298 K), N_2 (77 K) and Ar (77 K) reveal two steps with broad hysteresis while supercritical CH_4 (273 K) shows only one step and hysteresis. The unusual adsorption-desorption hysteresis loops were explained by a structural crystal-to-crystal-transition of the material indicating a third generation metal-organic framework as defined by Kitagawa et al.[5,6]

As mentioned before, pressure dependent *in situ* experiments, in particular X-ray powder diffraction are powerful tools to examine the flexibility of MOF materials as shown by several experiments[31,35-41]. Regarding that fact, C_4-hydrocarbon sorption at room temperature is predestined for *in situ* XRD studies due to the favorable physical properties: The low saturation vapor pressure at ambient temperature allows the coupling of the adsorption equipment to the X-ray diffractometer with little effort. This way diffraction data for any position in the adsorption isotherm up to the saturation pressure can be easily collected. In addition, C_4-hydrocarbons with linear or branched structure as well as paraffinic or olefinic character are an attractive series regarding a rigorous study of network flexibility. In comparison, N_2, CO_2 or Xe often require drastic conditions like cryogenic temperature or high pressure to investigate the whole isotherm including all structural transitions[31,35-41].

One goal of this study was to combine the measuring technique of XRD with a manometric adsorption equipment with the intention to prove and identify the pressure dependent structural flexibility *in situ*. Therefore, a commercial X-ray diffractometer was coupled with a gas supply keeping the procedure as simple as possible. Moreover, ancillary sorption experiments with C_4-hydrocarbons on **1** in a temperature range of 283 K – 343 K up to 300 kPa were performed by gravimetric sorption technique. From equilibrium sorption isotherms, thermodynamic parameters like the isosteric heat of adsorption, adsorption capacity and stability during C_4-hydrocarbon sorption are examined.

2. Experimental

2.1 $^{3}_{\infty}[Cu_4(\mu_4\text{-}O)(\mu_2\text{-}OH)_2(Me_2trz\text{-}pba)_4]$ (1)

The metal-organic framework $^{3}_{\infty}[Cu_4(\mu_4\text{-}O)(\mu_2\text{-}OH)_2(Me_2trz\text{-}pba)_4]$ (**1**) was prepared acc. to the procedure reported by Lincke et al.[42] refluxing the protonated ligand (Me_2trz-*p*ba)[44] and copper actetate hydrate in ethanol for 48 h (Scheme 1). The highest pore volume was achieved by postsynthetic Soxhlet extraction of the obtained solid with methanol and subsequent activation in vacuum. The single crystal structure **1**[42] possesses a three-dimensional pore system with two different windows and an estimated porosity of 57 % in total (calculated by PLATON/SQUEEZE-routine)[45]. The pore system contains windows of 450 x 550 pm in crystallographic *a* and *b* direction as well as 350 x 850 pm in *c* direction. After synthesis the textural properties of **1** were determined via sorption of N_2 at 77 K and of CO_2 at 298 K. As a result the adsorption-desorption isotherms regarding N_2 and CO_2 on **1** obtained in this study are the same as presented by Lincke et al.[42], confirming the same textural properties. A comparison of these data can be found in Table SI 1 in the Electronic Supplementary Information (ESI).

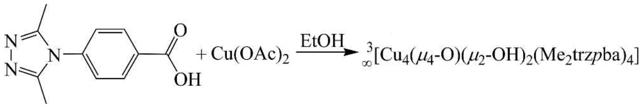

Scheme 1 Synthesis route of **1**.[42]

2.2 Adsorption experiments

2.2.1 C_4-Sorption measurements

The pure component adsorption of *n*-butane, isobutane, 1-butene and isobutene on **1** was measured in a temperature range from 283 to 343 K and at pressures up to 300 kPa using a magnetic suspension balance (Fa. Rubotherm GmbH, Bochum). Three pressure transducers (MKS Instruments Deutschland GmbH, Germany, Newport Omega Electronics GmbH, Germany) were used to gather accurate data from the whole pressure range up to 300 kPa.

In preparation of the sorption experiments, a stainless steel sample holder was typically filled with an amount 0.2 g of **1** and the balance was evacuated for at least 12 hours at 373 K and 0.3 Pa until constant mass was achieved. Subsequently the respective gas was dosed into the balance and pressure was increased after reaching the equilibrium. Adsorption equilibrium was assumed to be reached when no further weight increase within 15 minutes and constant pressure was observed. The temperature was kept constant with an accuracy of ± 0.5 K.

Gases were purchased from Linde or Air Products with purities of 99.5 % for *n*-butane, isobutane and 1-butene, 99.9 % for isobutene. The saturation vapor pressures of investigated C_4-hydrocarbons are listed in Table 1. Further gas properties of used gases are summarized in the Supporting Information (Table SI-2). In order to calculate the surface excess mass from the measured weight values, a buoyancy correction was carried out. A detailed description of this procedure can be found elsewhere[46]. The densities for each gas were calculated with the program *FLUIDCAL*[47].

2.2.2 Nitrogen and carbon dioxide adsorption

Nitrogen adsorption experiments at 77 K on **1** were conducted in the commercially available volumetric sorption analyzer BELSORP-max from Bel Japan Inc. with a high-resolution pressure sensor. For measurements, about 0.15 g of MOF material were filled into the sample cell and pre-treated at 373 K and a pressure below 0.05 Pa for 12 hours. The temperature was achieved by a heating rate of 5 K min^{-1}.

High pressure measurements of CO_2 and He sorption were performed using a magnetic suspension balance (Fa. Rubotherm GmbH, Bochum) up to 10 MPa. About 0.2 g were filled in a stainless steel sample holder and activated at 373 K and 0.3 Pa at least for 12 hours until no further decrease in weight was observed. Various pressure transducers (Newport Electronics GmbH, Germany) were used in a range of vacuum up to 10 MPa with an accuracy of 0.05 %. Gases were purchased from Linde or

Table 1 Saturation vapor pressures of used C_4-hydrocarbons in the temperature range 283 K-343 K.

T / K	p_0 / kPa			
	n-butane	isobutane	1-butene	isobutene
283.15	148.5	220.6	185.4	188.2
298.15	243.3	350.7	302.6	303.5
313.15	378.5	531.2	467.7	465.6
328.15	563.7	773.0	690.8	685.2
343.15	809.1	1087.5	982.3	974.3

Air Products with purities of 99.9992 % for nitrogen and 99.995 % for carbon dioxide. The surface excess mass was calculated from the measured weight by buoyancy correction.[46,47].

2.3 *In situ* XRD studies

A simple apparatus was built up for pressure dependent powder X-ray diffraction. A gas supply (Scheme 2) was coupled with a commercial X-ray diffractometer (Stadi P, STOE & Cie GmbH, Darmstadt, Germany) equipped with a sealed X-ray tube (Cu-$K_{\alpha1}$ radiation, $\lambda = 154.060$ pm) in Debye-Scherrer geometry. Microcrystalline **1** was filled into a 0.5 mm glass capillary as measuring cell ~~(glass capillary)~~ and activated by connection to a vacuum pump before each measurement. The adsorptive gas was admitted from a reservoir to the measuring cell through a dosing valve.

The measurements were carried out at room temperature at pressures up to 300 kPa for *n*-butane, isobutane, 1-butene and isobutene. The pressure in the cell was monitored over time by a pressure transducer (Newport Electronics GmbH, Germany). Equilibrium was assumed by observing a constant pressure within 5 minutes and at least after 30 minutes. Diffraction patterns were recorded at certain selected pressures known from the isotherm at 298 K.

3 Results and Discussion

3.1 Sorption properties of C_4-isomers on 1

In Fig. 1 and Fig. 2, the isotherms of *n*-butane and isobutane on **1** for 283 K, 313 K and 343 K are shown. The isotherms are presented in semi-logarithmic scale to point out details in the low pressure region. The isotherms measured for other temperatures are presented in Fig. SI 1 - Fig. SI 4. As already introduced by Lincke et al.[42] for CO_2, Ar and N_2 as sorptives, the curvature of the C_4-hydrocarbon sorption isotherms in this study does not correspond to any type of the IUPAC classification[48]. For all adsorptives investigated in this study, just a small increase of loading in the lower pressure region is observed which corresponds to a normal pore filling process of the first phase of **1**.

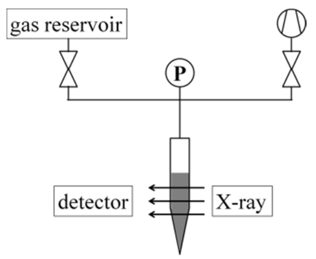

Scheme 2 Experimental set-up for pressure dependent XRD. Gas supply was combined with a commercial X-ray diffractometer. The sample could be evacuated directly in the measuring cell by connection to a vacuum pump.

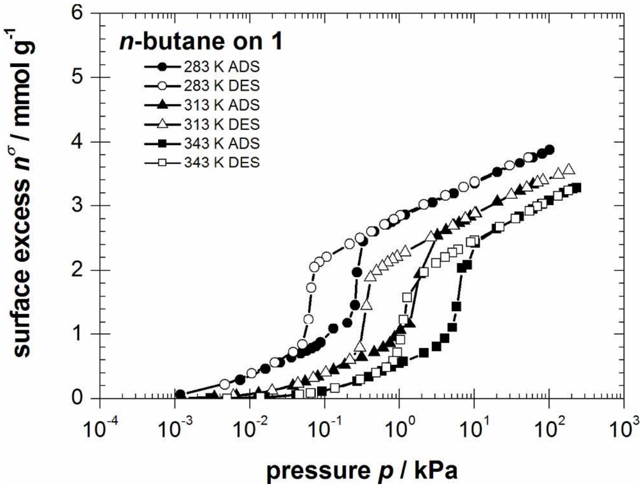

Fig. 1 Sorption isotherms of *n*-butane on **1** at 283 K (circles), 313 K (triangles) and 343 K (squares) – closed symbols denote adsorption (ADS) and open symbols desorption (DES).

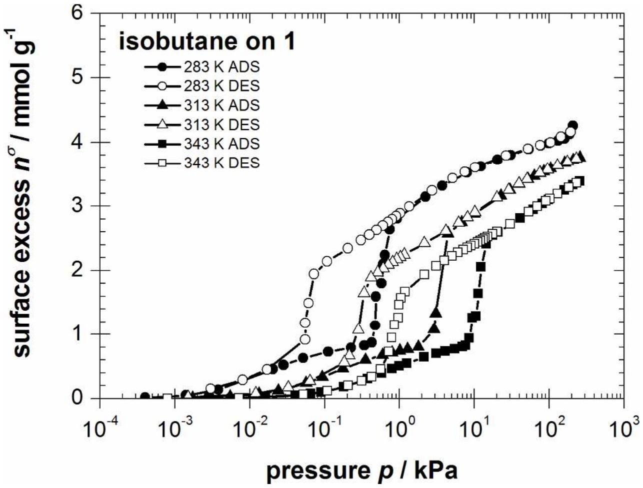

Fig. 2 Sorption isotherms of isobutane on **1** at 283 K (circles), 313 K (triangles) and 343 K (squares) – closed symbols denote adsorption (ADS) and open symbols desorption (DES).

After reaching a first plateau (more clearly seen in Fig. SI 7) the amount adsorbed rises spontaneously at a certain pressure and a second plateau is obtained. This pressure is for both C_4-hydrocarbons, *n*-butane and isobutane, on **1** studied in this work equal with a value of 0.5 to 1 kPa. At this pressure, a structural transformation is assumed which includes changes in pore size and offers a larger pore volume resulting in higher amounts adsorbed. This gate opening pressure depends on temperature, sorptive and adsorbent. The desorption branch coincides with the adsorption branch at pressures above the gate opening pressure. By decreasing the pressure below the gate opening pressure the loading remains up to a pressure of 0.08 to 0.12 kPa at 283 K, which is called the gate closing pressure, where the isotherm shows a sudden decrease. The completely reversible adsorption behaviour observed indicates a reversible crystal-to-crystal-transformation of the framework.

In general, the same behavior can be observed for the sorption of 1-butene and isobutene, presented in Fig. 3 and 4. In contrast to *n*-butane and isobutane, for 1-butene a second broad hysteresis loop is observed at a pressure of 100 kPa ($p/p_0 = 0.54$) up to 175 kPa ($p/p_0 = 0.94$) at 283 K, i.e., close to the saturation pressure. A similar hysteresis was also found at 298 K (cf. Fig. SI 3). We interpret this with respect to the classification of Coudert et al.[41] as an additional structural transition of **1** resulting in a higher pore volume and, thus, in higher loadings for 1-butene on **1** at pressures above 100 kPa at 283 K.

Similarly to *n*-butane and isobutane, a second broad hysteresis is not observed for sorption of isobutene. However, the isotherm of isobutene at 283 K (Fig. 4) shows another small hysteresis at 1 - 3 kPa next to the broad one, although less pronounced than for 1-butene. This small hysteresis is not observed at higher temperatures. Similarly, Coudert et al.[49] presented temperature-dependent xenon adsorption on the MOF MIL-53(Al) concluding that in a specific temperature range two phase transitions can occur (large pore – narrow pore – large pore). Nevertheless, for higher temperatures above 300 K only one or even no phase transition was assumed in case of MIL-53(Al). The behavior of **1** regarding isobutene adsorption can be interpreted in a similar way. The small hysteresis loop between 1 and 3 kPa at 283 K can also be found in the 313 K sorption isotherm in the pressure range of 4 to 8 kPa. At this temperature the step in the isotherm is significantly lower, whereas at 343 K this transition disappears. Referring to the situation of Xe adsorption in MIL-53(Al), in a resulting phase diagram **1** shows a comparable temperature dependence[49].

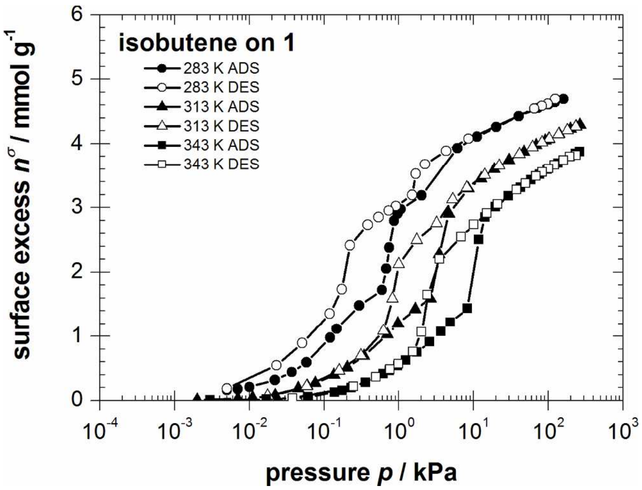

Fig. 4 Sorption isotherms of isobutene on **1** at 283 K (circles), 313 K (triangles) and 343 K (squares) – closed symbols denote adsorption (ADS) and open symbols desorption (DES).

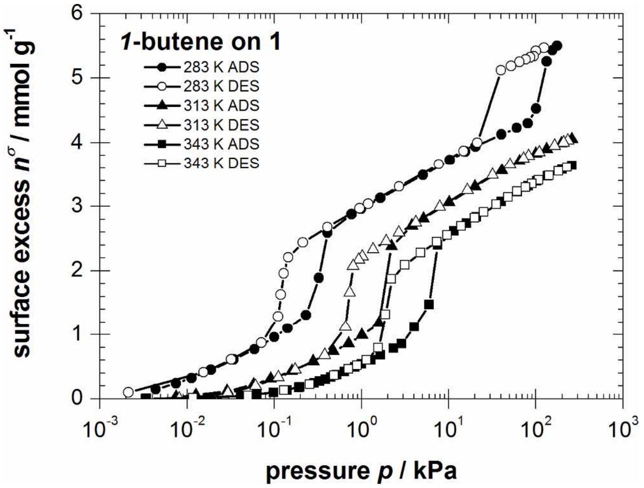

Fig. 3 Sorption isotherms of 1-butene on **1** at 283 K (circles), 313 K (triangles) and 343 K (squares) – closed symbols denote adsorption (ADS) and open symbols desorption (DES).

All sorption isotherms exhibit the expected temperature dependence for loading, i.e., the amount adsorbed is lower forhigher temperatures. In the same way, the hysteresis is shifted to higher pressures with increasing temperature. By comparing the loadings at 283 K (cf. Fig. SI 5), it becomes obvious that adsorption of *n*-butane, isobutane, 1-butene and isobutene are different in the low pressure region before the first phase transition takes place. At a pressure of around 0.3 to 1 kPa, isobutene has the highest amount adsorbed with 1.8 mmol g^{-1} followed by 1-butene with 1.3 mmol g^{-1}, *n*-butane with 1.2 mmol g^{-1} and isobutane with 0.8 mmol g^{-1}, respectively. For the second plateau, at a pressure of 100 kPa at 283 K, where one transition step occurred, the amount adsorbed is different compared to the situation at lower pressures. The highest loading is achieved for isobutene with 4.6 mmol g^{-1}, followed by 1-butene, isobutane and *n*-butane with loadings of, 4.4 mmol g^{-1}, 4.0 mmol g^{-1} and 3.8 mmol g^{-1} at 283 K and $p/p_0 = 0.67$, respectively. At pressures above 100 kPa ($p/p_0 > 0.70$), the adsorption of 1-butene causes a second structural transformation resulting in an additional hysteresis loop and a higher amount adsorbed of 5.3 mmol g^{-1}. For higher temperatures, this second step in the 1-butene isotherm on **1** was not observed due to the low relative pressures applied in this study. However, under ambient conditions (298 K and 100 kPa) the isobutene sorption capacity on **1** is the highest compared to the other C_4-hydrocarbons investigated. For a better comparison some C_4-sorption data on **1** and several other materials under similar conditions are listed in Table 2.

The sorption capacity of **1** for C_4-hydrocarbons under ambient conditions is relatively low compared to some other MOF materials, especially to mesoporous materials like DUT-6[51] as expected regarding its larger pore volume. Nevertheless, the amount adsorbed of *n*-butane is comparable to that of the flexible MIL-53 family[36] and activated carbons (F30/470)[58]. In contrast, the *n*-butane sorption capacity on **1** is significantly higher than that of zeolites. This is due to the fact that at 298 K and 100 kPa the adsorption isotherm is near the saturation regime and the loading is only influenced by the overall available pore volume.

As already shown by Lincke et al.[32] for adsorption of N_2, Ar, CO_2, MeOH and CH_4, the gate opening of **1** depends on the sorptive, on the temperature and on the pressure. For a detailed comparison with C_4-hydrocarbons, studied here, gate opening pressures were taken from the corresponding isotherms for the first broad hysteresis at low pressures, e.g., at 283 K of around 0.3 to 1 kPa. As a result, in Fig. 5 the gate opening pressure as a function of temperature for each C_4-hydrocarbon indicating the

Table 2 Conditions and loadings of C_4-hydrocarbon sorption on different materials including activated carbons, zeolites and MOFs.

adsorptive	adsorbent	Temperature / K	pressure / kPa	loading / mmol g^{-1}	ref.
n-butane	**1**	298	102.4	3.78	this study
	$Cu_3(BTC)_2$		108.6	5.98	50
	DUT-6(Zn)		101.0	18.24	51
	DUT-8(Ni)			5.76	52
	DUT-9(Ni)			11.37	53
	DUT-13(Zn)			6.87	54
	AC (Kureha)			5.30	55
	AC (Maxsorb III)			12.20	56
	MIL-53(Cr)	303	101.0	3.89	36
	MIL-53(Fe)		99.7	2.79	
	ZSM-5		100.0	1.70	57
	AC (F30/470)	293	110.1	3.77	58
isobutane	**1**	298	100.7	3.83	this study
	$Cu_3(BTC)_2$	323	98.8	5.97	59
	zeolite 13X	298	90.5	1.81	60
	AC (F30/470)	293	105.9	3.39	58
1-butene	**1**	298	99.7	4.10	this study
	AC (F30/470)	293	106.2	4.04	58
isobutene	**1**	298	103.4	4.35	this study
	$Cu_3(BTC)_2$	298	108.6	5.98	50

first crystal-to-crystal transformation is presented. It is obvious, that linear C_4-hydrocarbons open the framework of **1** at lower gate opening pressures compared to their branched isomers. The gate opening pressure for all adsorptives on **1** increases with temperature. The difference between linear and branched isomers is quite small at low temperatures, but expands for higher temperatures, e.g., at 343 K, where the differences lie between 6 kPa for 1-butene and *n*-butane and 10 to 12 kPa for isobutene and isobutane, respectively.

The pore volumes of **1** were calculated by means of the Gurvich rule[61,62] from the adsorption isotherms at pressures before and after the hysteresis loop with the condition that a plateau is reached. The calculated pore volumes at 283 K are given in Table 3. The pore volumes of **1** are 0.09 $cm^3\ g^{-1}$ after the first pore filling with paraffinic isomers and 0.13 - 0.16 $cm^3\ g^{-1}$ for the olefinic analogues. These values for *n*-butane and isobutane are similar to the pore volumes of **1** given by Lincke et al.[42] for the pore filling at lower pressures, i.e., before the first structural transition, regarding the adsorption of CO_2 at 273 K and 298 K, Ar at 77 K, CH_3OH at 298 K or N_2 at 77 K. In the region of saturation pressure ($p/p_0 > 0.68$) the pore volumes for *n*-butane, isobutane and isobutene are almost equal with values of 0.40 $cm^3\ g^{-1}$, 0.42 $cm^3\ g^{-1}$ and 0.43 $cm^3\ g^{-1}$, respectively. Solely 1-butene seems to open the framework completely resulting in a significantly higher calculated pore volume of 0.54 $cm^3\ g^{-1}$ at $p/p_0 = 0.94$. This value of the total pore volume is in good agreement with the total pore volumes given by Lincke et al.[42], i.e., 0.53 $cm^3\ g^{-1}$ for CO_2 adsorption at 273 K, 0.52 $cm^3\ g^{-1}$ for Ar at 77 K or 0.58 $cm^3\ g^{-1}$ for N_2 adsorption at 77 K, CH_3OH adsorption at 298 K as well as CO_2 adsorption at 298 K, respectively (Table 3). Furthermore, these values are nearly identical to the pore volume determined from single crystal structure data (0.59 $cm^3\ g^{-1}$)[42].

As is evident from Table 3, sorption of C_4-hydrocarbons is comparable to that of other sorptives before structural transition of the framework of **1**. However, for *n*-butane, isobutane and

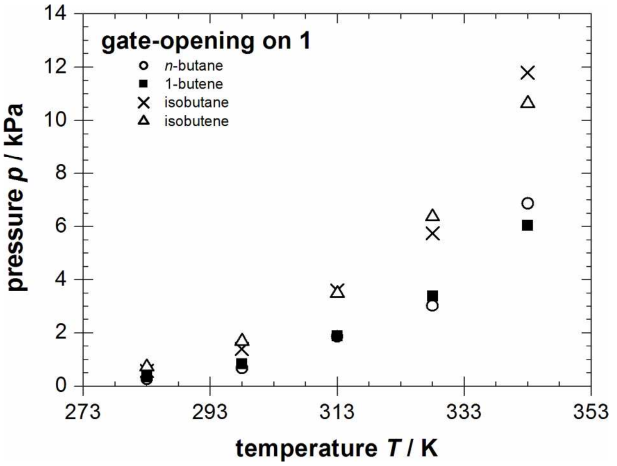

Fig. 5 Temperature dependent gate opening pressures for adsorption of *n*-butane, 1-butene, isobutane and isobutene on **1** in linear (left) and logarithmic scale (right).

Table 3 Pore volumes of **1** for C_4-sorptives calculated from experimental isotherms by Gurvich rule[61,62].

	After 1st pore filling		After 1st transition	
	p/p_0	V_{pore} / $cm^3\ g^{-1}$	p/p_0	V_{pore} / $cm^3\ g^{-1}$
N_2 at 77 K[42]	0.001	0.16	0.90	0.58
CO_2 at 273 K[42]	0.050	0.13	0.90	0.53
CO_2 at 298 K[42]	0.030	0.13	0.60	0.58
n-butane at 283 K	0.001	0.09	0.68	0.40
isobutane at 283 K	0.002	0.09	0.88	0.42
1-butene at 283 K	0.001	0.13	0.94	0.41[1]; 0.54[2]
isobutene at 283 K	0.003	0.16	0.85	0.43

[1] After 1st transition, [2] After 2nd transition

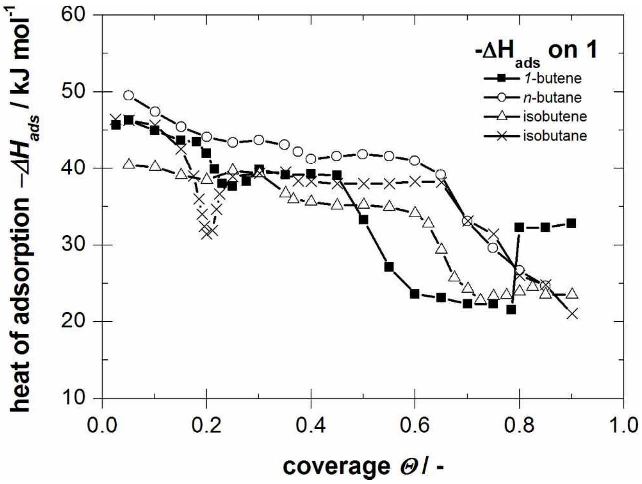

Fig. 6 Heat of adsorption as a function of coverage for sorption of *n*-butane, 1-butene, isobutane or isobutene on **1**.

isobutene only one phase transition is observed (cf. Fig. 1, 2 and 4) and, thus, a smaller pore volume can be determined. Only 1-butene sorption exhibits a second broad hysteresis in saturation pressure region at 283 K (cf. Fig. 3), which certainly leads to a higher pore volume comparable to the theoretical value.

3.2 Isosteric heat of adsorption

The isosteric heat of adsorption ($-\Delta H_{ads}$) of *n*-butane, isobutane, 1-butene as well as isobutene on **1** were calculated from the experimental data, i.e. coverage as a function of pressure for different temperatures using Clausius-Clapeyron equation[63]. Intermediate values were interpolated (cf. Fig. SI 6).

$$\frac{-\Delta H_{ads}}{R} = \left(\frac{\partial \ln P}{\partial (1/T)}\right)_{\Theta} \qquad (1)$$

The coverage Θ was determined by equation (2) with maximum loading (n_{max}) for each temperature at $p/p_0 = 0.99$.

$$\Theta = \frac{n}{n_{max}} \qquad (2)$$

From Fig. 6 it becomes obvious, that the isosteric heat of adsorption on **1** is in a close region between 40 and 50 kJ mol^{-1} for all adsorptives at zero coverage and expectedly decreases with higher coverage. The heat of adsorption of *n*-butane on **1** is the highest for coverage up to $\Theta = 0.8$. Regarding low coverages until $\Theta = 0.2$, the lowest value is observed for isobutene. However, between $\Theta = 0.2$ and $\Theta = 0.6$ it just decreases slightly for all sorptives assuming a dependence on the gate opening process which generates new sorption sites. A peculiarity is observed for isobutane, where a sharp minimum in the isosteric heat of adsorption is observed at a coverage of $\Theta = 0.2$. This is a result of the reached well-defined plateau in the sorption isotherm indicating a nearly complete pore filling of **1**, before the first crystal-to-crystal transformation occurs (cf. Fig 2). This results in the striking drop in the heat of adsorption at coverage of $\Theta = 0.2$ due to reduced interaction between sorptive and adsorbent surface. While the gate opening proceeds, new adsorption sites are generated and occupied by adsorptive molecules resulting in an increase of the isosteric heat of adsorption. For the other sorptives this effect is indistinct because the isotherms do not show such a defined saturation plateau for first pore filling followed by a sharp rise of loading. Here, energetically equal sorption sites are available during the whole sorption process until the first structural transformation occurs. For 1-butene adsorption, a second gate opening at higher pressures was observed in the isotherm, which again leads to an increase of the isosteric heat of adsorption at higher coverage (θ = 0.8).

In addition, the isosteric heat of adsorption was determined by fitting the data points before the first structural transition, in particular before the gate opening pressure was reached, with the Langmuir model[64] (cf. Fig. SI 7) in combination with Clausius-Clapeyron equation[63]. These results are compared to several other materials in Table 4. Langmuir parameters of the fits are listed in Table SI 2. The comparison of the adsorption enthalpies in Fig. 6 and Table 4 shows that data determined by both methods used in this study are in good agreement.

The isosteric heat of adsorption is especially in low pressure range a degree for interaction between adsorptive and adsorbent surface. The values of **1** are generally in the range of that for

Table 4 Isosteric heat of adsorption for different adsorptives on various adsorbents including MOFs, activated carbons and zeolites (Langmuir model).

adsorbent	**adsorptive**	**$-\Delta H_{ads}$ / kJ mol^{-1}**	**refs.**
1	*n*-butane	49.5[1]; 50.2[2]	this study
	isobutane	46.4[1]; 49.3[2]	
	1-butene	45.6[1]; 49.1[2]	
	isobutene	40.4[1]; 43.5[2]	
$Cu_3(BTC)_2$	*n*-butane	35.6	65
	isobutane	31.7	
	isobutane	42.0	50
	isobutene	46.0	
MIL-53(Cr)	*n*-butane	46.8	66
amino-MIL-53(Al)	*n*-butane	42.9	67
AC (Kureha)	*n*-butane	46.3	55
AC (Maxsorb III)	*n*-butane	52.0-56.0	56
NaCaA	*n*-butane	32.0	57
ZSM-5 (Si/Al = 150)	*n*-butane	60.0	57
zeolite 13X	isobutane	39.3	60

[1] exp. Data + Clausius-Clapeyron, [2] Langmuir + Clausius-Clapeyron.

activated carbons and other MOF materials like MIL-53(Cr) or even higher as in case of $Cu_3(BTC)_2$. This might be a consequence of small, tight pores in the first phase of sorption, i.e. before the structural change by gate opening. Zeolites with high Si/Al-ratios are hydrophobic and consequently, values for *n*-butane sorption are higher (60.0 kJ mol^{-1}, cf. Table 4, ZSM-5) than for **1** (around 50 kJ mol^{-1}. Besides other zeolite materials exhibit a lower isosteric heat of adsorption, e.g. zeolite 5A (NaCaA) with 39.3 kJ mol^{-1} compared to **1**.

3.3 *In situ* XRD studies

After activation, i.e. the removal of guest molecules, **1** shows sufficient crystallinity for qualitative observation of changes in the X-ray diffraction pattern. However, due to reduced crystallinity, the quality of the diffraction pattern is not good enough for structure solution. Hence, it was possible to monitor structural changes by means of changes in the ~~X-ray~~ diffraction pattern during C_4-hydrocarbon sorption on **1** at room temperature up to saturated vapor pressures. Fig. 7 presents the pressure dependent X-ray diffraction patterns of **1** at different loadings with 1-butene. A small aperture for 2θ between 6 ° and 12 ° is chosen because the material shows the strongest reflections in this range (cf. Fig. SI 8). Hence, changes in the diffraction pattern due to structural changes can be pointed out most sensitively in this region. At certain pressures, powder patterns were recorded corresponding to different C_4-hydrocarbon loadings.

From the diffraction patterns it can be concluded that for low loadings the structure is similar to that of the evacuated material (cf. Fig 7, points 1 and 2). Thus, there are two strong reflections (2θ = 7.5 ° and 8.7 °) and a weak one (9.4 °). With increasing 1-butene pressure, the pattern changes according to a structural change starting at 1.2 kPa (point 3). Disappearing and new formation of reflections indicates a structural change.

There might be a coexistence of two structures over a certain pressure range (points 3 and 4). At a pressure of about 75 kPa, the newly formed phase is present (points 5 and 6). Whereas the reflection at 7.5 ° disappears during adsorption, a new reflection appears at 7.7 °. In addition the peak at 8.7 ° is shifted with increasing pressure to 8.5 ° (points 1-3) and disappears at 10.33 kPa (point 4). In contrast, beginning at 1.20 kPa a new reflection is observed at 8.8 ° which is also shifted to lower diffraction angles (points 3-7). Since the diffraction patterns of point 1 (0.25 kPa) and point 5 (76.45 kPa) are completely unrelated, structural changes, corresponding to a gate opening process, are clearly evident. In particular, the pattern at point 3 shows reflections of both phases of point 2 and point 4. Thus the coexistence of particles/domains of the evacuated phase and the phase after the first gate opening is proved. For 1-butene, a second gate opening is observed above 210 kPa. In the associated pattern at 290 kPa (point 7), an additional peak appears at 7.2 °. This pattern resembles that of the solvated material obtained after Soxhlet extraction of the as-synthesized MOF material **1** with methanol (cf. Fig. SI 9). This indicates that 1-butene is able to induce structural transformations and reformation of the structure of the as-synthesized material indicated by powder patterns similar to the pristine MOF filled with methanol. As a conclusion, during the adsorption of 1-butene at 283 K the framework of **1** undergoes a crystal-to-crystal reformation according to Kitagawa`s type III category[5,6]. Contrary, the adsorption of isobutene, isobutane and *n*-butane does not cause a complete reformation. As a result, this observation makes it difficult to classify flexible metal-organic frameworks only with respect to their types of adsorption isotherms, in particular, materials like **1** can be assigned to more than one type.

The powder diffraction patterns corresponding to points on the desorption branch, show ~~similar~~ comparable changes in positions and intensities of the XRD reflections. The open phase (point 7) is present to 118.4 kPa (point 8). With decreasing pressure, the reflections at 7.2° and 8.2° disappear, whereas the one at 8.7° is shifted to higher diffraction angles. This transition reveals the second hysteresis in the isotherm. As a result, the pattern at 76.5 kPa (point 10) is similar to that of point 5 in the adsorption branch. After another framework transformation evidenced by changes in the powder pattern (points 11-14), the evacuated phase is equal to the activated phase present before the adsorption experiment. This illustrates the reversibility of the gate opening. Since the powder pattern of the activated phase is re-obtained after the sorption experiment, it can be assumed that the

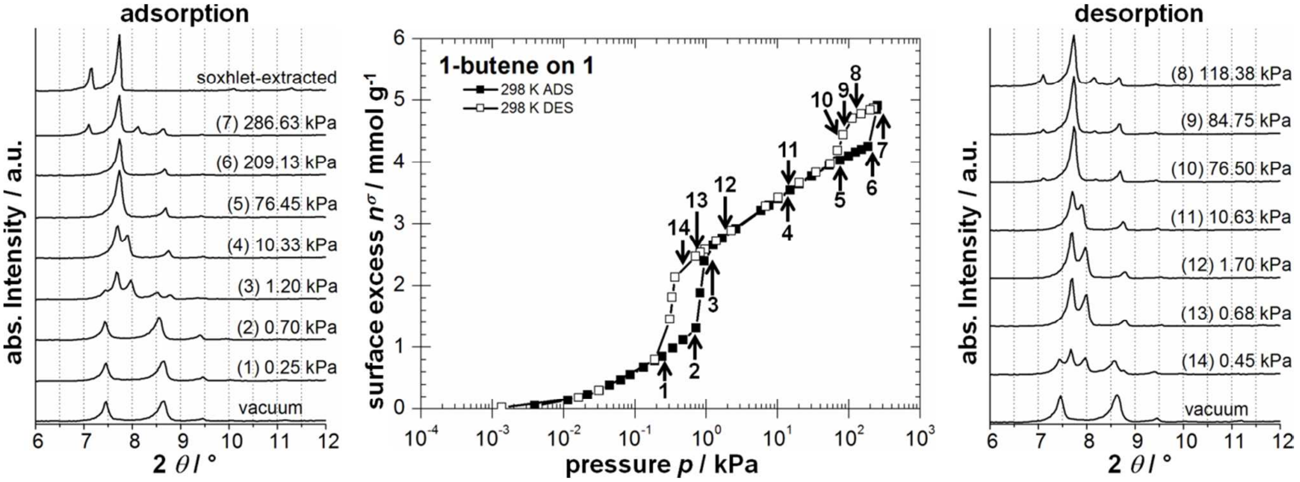

Fig. 7 Adsorption (closed symbols) and desorption (open symbols) isotherm of 1-butene on **1** (center) at 298 K and XRD patterns of **1** at different pressures for adsorption (left) and desorption (right). The respective points on the sorption isotherms at which the XRD patterns were recorded are labelled as 1 – 14. The first gate opening is observed at about 1 kPa (point 2). For 1-butene a second gate opening occurs at around 210 kPa.

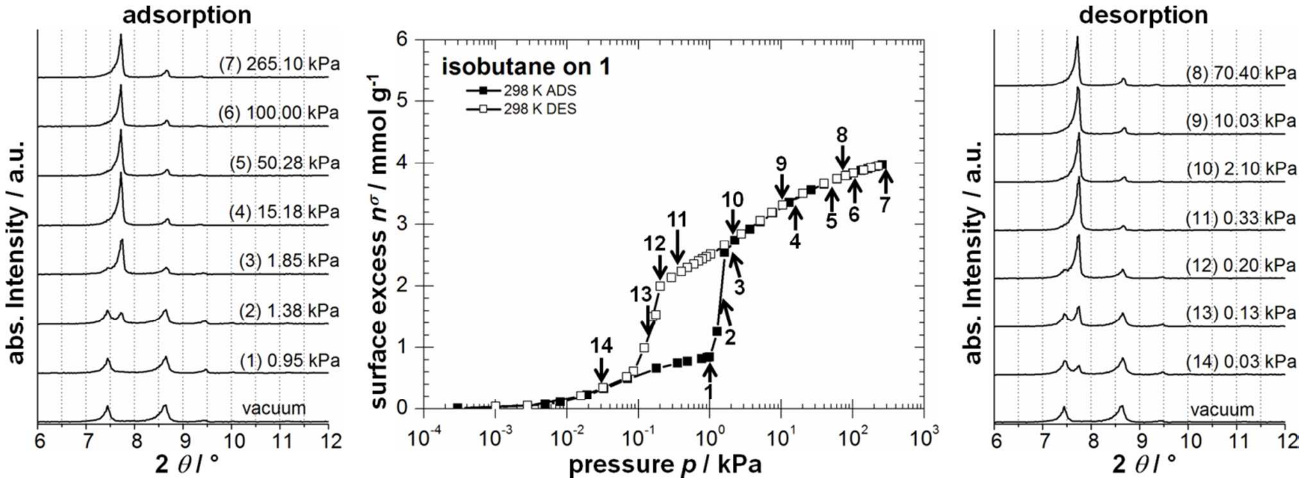

Fig. 8 Adsorption (closed symbols) and desorption (open symbols) isotherm of isobutane on **1** (center) at 298 K and XRD patterns of **1** at different pressures for adsorption (left) and desorption (right). The respective points on the sorption isotherms at which the XRD patterns were recorded are labelled as 1 – 14. The gate opening is observed at about 1 kPa (point 1).

framework topology is not changing during the gate opening and -closing process.

The pressure dependent XRD patterns for isobutane at 298 K are shown in Fig. 8. Similar to the adsorption of 1-butene the uptake of isobutane causes a structural change starting at 1.38 kPa (point 2). The change of the powder pattern is quiet sharp in a small pressure range corresponding perfectly to its isotherm at 298 K. Transformation leads to a defined structure for higher pressures (points 3-7). The corresponding XRD pattern of this form exhibits one intense peak at 7.7 ° and a weak one at 8.6 ° and resembles point 5 of the 1-butene adsorption. Thus it can be concluded that the gate opening process is the same for 1-butene and isobutene. In addition, the reformation of the evacuated powder pattern evidences the reversibility of the structural change. This gate opening is also observed during the adsorption of isobutene and *n*-butane, starting at particular pressures. The low pressure phase is present up to sorptive specific pressures: 0.28 kPa for isobutene, 0.48 kPa for *n*-butane, 0.7 kPa for 1-butene and 0.95 kPa for isobutane, respectively. As a consequence, subsequently to these pressures a structural change occurs, which results in a not yet elucidated structural motive over a certain pressure range. This is again detected for all C_4-hydrocarbons on **1** at specific pressures. In particular, this pattern is already observed at a pressure of 1.85 kPa for isobutane adsorption and during 1-butene adsorption it shows up at 76.5 kPa. For adsorption of *n*-butane and isobutene it is detected at pressures of 25.5 kPa and 10.0 kPa, respectively. Similar to the 1-butene and isobutane studies the structural change observed for isobutene and *n*-butan is completely reversible. The XRD patterns and associated isotherms of *n*-butane and isobutene at 298 K are given in the ESI (Fig. SI 10 and 11).

Only the XRD patterns of **1** for adsorption of 1-butene at 298 K and pressures above 250 kPa show another structural change (Fig. SI 9). However, no further structural changes in this pressure region are expected for the other C_4-isomers measured in this study. This can be concluded based on their isotherms at 283 K (cf. Fig. 1-4 and SI 5) which were obtained up to respective vapor saturation pressures.

3.4 Stability of the material

In order to investigate any effect of C_4-hydrocarbon sorption on **1**, its textural properties measured by N_2 sorption at 77 K and CO_2 sorption at 298 K before and after sorption experiments are compared (Fig. 9 and Fig. SI 12). They are consistent with the data reported by Lincke et al.[42]

Within the whole study, the material does not show any loss of adsorption capacity. In addition, the structural flexibility of the framework remains unaffected after the sorption experiments. Moreover, gate opening and gate closing pressures remain unchanged. This is consistent with the observations by Lincke et al.[42]: the XRD pattern of **1** changes after CO_2 sorption, but after resolvatisation with methanol, the original diffraction pattern is restored. In addition, Reichenbach et al.[43] reported that this flexible material is sensitive to external stimuli and must be handled with care. Exposure of the sample to moist air leads to a certain reduction of pore volume and network flexibility. In the present study, the material overcomes 20 sorption and activation cycles (vacuum combined with heating up to 373 K). No negative influence on the adsorption performance of **1** was observed.

4. Conclusions

Adsorption isotherms of the C_4-hydrocarbons *n*-butane, isobutane, 1-butene and isobutene were determined by gravimetric sorption experiments in a temperature range of 283 - 343 K at pressures up to 300 kPa on the copper-based MOF $^{3}_{\infty}[Cu_4(\mu_4\text{-}O)(\mu_2\text{-}OH)_2(Me_2trz\text{-}pba)_4]$ (**1**). The resulting isotherms are typical of flexible MOFs and do not correspond to the classification of the IUPAC for rigid porous materials. By comparing the sorption isotherms of the studied C_4-hydrocarbons a first gate opening is observed at lower pressures, whereas at higher pressures only 1-butene shows an additional sharp increase in loading. The gate opening pressure increases with increasing temperature. For linear C_4-isomers, the gate opening pressures are lower compared to their branched analogues.

Pore volumes of **1**, as obtained by Gurvich's rule for the different adsorptive, are comparable before gate opening occurs; from C_4-

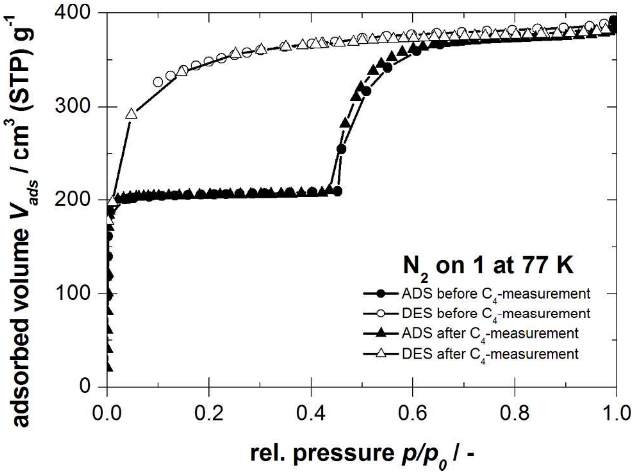

Fig. 9 Sorption isotherms of nitrogen at 77 K on **1** before and after experiments with C_4-hydrocarbons.

hydrocarbon sorption a pore volume of 0.09 to 0.16 cm^3 g^{-1} was calculated, which is in accordance to N_2 and CO_2 sorption. After gate opening, the pore volumes calculated for sorption of *n*-butane, isobutene and isobutene (around 0.43 cm^3 g^{-1}) are much lower than for 1-butene. For 1-butene the pore volume (around 0.54 cm^3 g^{-1}) is close to that calculated from single crystal structure data for the fully accessible pore system.

The interaction of C_4-hydrocarbons with **1** can be described by the isosteric heat of adsorption, which is in a close range between 41 and 49 kJ mol^{-1} at low coverage. Conspicuous up-and-down trends in isosteric heat of adsorption are due to the structural transitions.

In situ XRD measurements were carried out with **1** during adsorption of *n*-butane, isobutane, 1-butene and isobutene at 298 K up to 300 kPa. It becomes obvious that different loadings with C_4-hydrocarbons result in different XRD patterns. Hence, it is proven by a combination of sorption studies with XRD analysis that structural changes occur during sorption of gaseous hydrocarbons on **1** corresponding to reversible framework flexibility. Contrary to the other sorptives, 1-butene leads to a second pore opening in the structure of **1**. From that only 1-butene affected a complete crystal-to-crystal reformation of the structure of the as-synthesized material, whereas the adsorption of isobutane, isobutene and *n*-butane only leads to a partial reformation. The structural changes are accompanied by disappearance and new formation of reflections in the XRD pattern. During the adsorption and desorption runs the framework topology does not change.

We are currently investigating details of the structural transformation/reformation process. Further *in situ* sorption measurements with CO_2 and N_2 at low temperatures in combination with theoretical studies shall give additional insights.

Acknowledgement

We thank the Deutsche Forschungsgemeinschaft (DFG SPP 1362 – Poröse metallorganische Gerüstverbindungen, STA 428/17-2 KR 1675/7-2 and GL 290/6-2) for financial support. The University of Leipzig (PbF-1), and the graduate school BuildMoNa are gratefully acknowledged. D.L. acknowledges the fellowship of the Fonds der Chemischen Industrie. J.L. is grateful for an ESF fellowships. This work was funded by the European Union and the Free State of Saxony.

Notes and references

[a] *Institut für Nichtklassische Chemie e.V., Permoserstr. 15, D-04318 Leipzig, Germany. E-mail: glaeser@inc.uni-leipzig.de; Fax: +49 (0)341 235 2701; Tel: +49 (0)341 235 2445*
[b] *Universität Leipzig, Fakultät für Chemie und Mineralogie, Johannisallee 29, D-04103 Leipzig, Germany. E-mail: krautscheid@rz.uni-leipzig.de; Fax: +49 (0)341 9736199; Tel: +49 (0)341 9736172*
[c] *Hochschule Offenburg, Fakultät Maschinenbau und Verfahrenstechnik, Badstraße 24, D-77652 Offenburg, Germany. E-mail: Reiner.Staudt@fh-offenburg.de; Tel: +49 (0)781 205 161*

† Electronic Supplementary Information (ESI) available: Physical properties of used gases, fitting data as well as experimental data are available in the ESI. See DOI: 10.1039/b000000x/

1 W.G. Klemperer, T.A. Marquart, O.M. Yaghi, *Angew. Chem. Int. Ed.*, 1992, **31**, 49-51.
2 M. Eddaoudi, D.B. Moler, H. Li, B. Chen, M. O'Keeffe, O.M. Yaghi, *Acc. Chem. Res.*, 2001, **34**, 319-330.
3 O.M. Yaghi, M. O'Keeffe, N.W. Ockwig, H.K. Chae, M. Eddaoudi, J. Kim, *Nature*, 2003, **423**, 705-714.
4 S.L. James, *Chem. Soc. Rev.*, 2003, **32**, 276-288.
5 S. Kitagawa, M. Kondo, *Bull. Chem. Soc. Jpn.*, 1998, **71**, 1739-1753.
6 S. Kitagawa, R. Kitaura, S. Noro, *Angew. Chem. Int. Ed.*, 2004, **43**, 2334-2375.
7 L.E. Kreno, K. Leong, O.K. Farha, M. Allendorf, R.P. Van Duyne, J.T. Hupp, *Chem. Rev.*, 2012, **112**, 1105-1125.
8 G. Lu, J.T. Hupp, *J. Am. Chem. Soc.*, 2010, **132**, 7832-7833.
9 S. Achmann, G. Hagen, J. Kita, I.M. Malkowsky, C. Kiener, R. Moos, *Sensors*, 2009, **9**, 1574-1589.
10 F.X. Llabres i Xamena, A. Abad, A. Corma, H. Garcia. *J. Cat.*, 2007, **250**, 294-298.
11 T. Uemura, N. Yanai, S. Kitagawa, *Chem. Soc. Rev.*, 2009, **38**, 1228-1236.
12 L. Ma, C. Abney, W. Lin, *Chem. Soc. Rev.*, 2009, **38**, 1248-1256.
13 D. Farrusseng, S. Aguado, C. Pinel, *Angew. Chem. Int. Ed.*, 2009, **48**, 7502-7513.
14 F. Kettner, C. Worch, J. Möllmer, R. Gläser, R. Staudt, H. Krautscheid, *Inorg. Chem.*, 2013, **52**, 8738-8742.
15 A.U. Czaja, N. Trukhan, U. Müller, *Chem. Soc. Rev.*, 2009, **38**, 1284-1293.
16 L.J. Murray, M. Dincà, J.R. Long, *Chem. Soc. Rev.*, 2009, **38**, 1294-1314.
17 J. Yang, A. Sudnik, C. Wolverton, D.J. Siegel, *Chem. Soc. Rev.*, 2010, **39**, 656-675.
18 M. Hirscher, B. Panella, B. Schmitz, *Micropor. Mesopor. Mater.*, 2010, **129**, 335-339.
19 M. Bastos-Neto, C. Patzschke, M. Lange, J. Möllmer, C. Schrage, D. Lässig, J. Lincke, R. Staudt, H. Krautscheid, R. Gläser, *Energy Environ. Sci.*, 2012, **5**, 8294- 8303.
20 P.S. Barcia, L. Bastin, E.J. Hurtado, J.A.C. Silva, A.E. Rodrigues, B. Chen, *Sep. Sci. Technol.*, 2008, **43**, 3494-3521.
21 J.-R. Li, R.J. Kuppler, H.-C. Zhou, *Chem. Soc. Rev.*, 2009, **38**, 1477-1504.
22 L. Hamon, P.L. Llewellyn, T. Devic, A. Ghoufi, G. Clet, V. Guillerm, G.D. Pirngruber, G. Maurin, C. Serre, G. Driver, W. van Beek, E. Jolimaitre, A. Vimont, M. Daturi, G. Ferey, *J. Am. Chem. Soc.*, 2009, **131**, 17490-17499.
23 P.S. Barcia, D. Guimaraes, P.A.P. Mendes, J.A.C. Silva, V. Guillerm, H. Chevreau, C. Serre, A.E. Rodrigues, *Micropor. Mesopor. Mater.*, 2011, **139**, 67-73.
24 A.F.P. Ferreira, J.C. Santos, M.G. Plaza, N. Lamia, J.M. Loureiro, A.E. Rodrigues, *Chem. Eng. J.*, 2011, **167**, 1-12.

25 F. Debatin, J. Möllmer, S.S. Mondal, K. Behrens, A. Möller, R. Staudt, A. Thomas, H.-J. Holdt, *J. Mater. Chem.*, 2012, **22**, 10221-10227.

26 J. Möllmer, A. Möller, C. Patzschke, K. Stein, D. Lässig, J. Lincke, R. Gläser, H. Krautscheid, R. Staudt, *J. Mater. Chem.*, 2012, **22**, 10274-10286.

27 D. Li, K. Kaneko, *Chem. Phys. Lett.*, 2001, **335**, 50-56.

28 G. Chaplais, A. Simon-Masseron, F. Porcher, C. Lecomte, D. Bazin-Bachi, N. Bats, J. Patarin; *Phys. Chem. Chem. Phys.*, 2009, **11**, 5241-5245.

29 R. Kitaura, K. Seki, G. Akiyama, S. Kitagawa, *Angew. Chem. Int. Ed.*, 2003, **42**, 428-431.

30 H. Kanoh, A. Kondo, H. Noguchi, H. Kajiro, A. Tohdoh, Y. Hattori, W.C. Xu, M. Moue, T. Sugiura, K. Morita, H. Tanaka, T. Ohba, K. Kaneko, *J. Colloid Interface Sci.*, 2009, **334**, 1–7.

31 S. Couck, E. Gobechiya, C.E.A. Kirschhock, P. Serra-Crespo, J. Juan-Alcañiz, A. Martinez Joaristi, E. Stavitski, J. Gascon, F. Kapteijn, G.V. Baron, J.F.M. Denayer, *Chem. Sus. Chem.*, 2012, **5**, 740–750.

32 F. Millange, C. Serre, G. Férey, *Chem. Commun.*, 2002, 822-823.

33 T. Loiseau, C. Serre, C. Huguenard, G. Fink, F. Taulelle, M. Henry, T. Bataille, G. Ferey, *Chem. Eur. J.*, 2004, **10**, 1373-1382.

34 C. Serre, F. Millange, C. Thouvenot, M. Nogues, G. Marsolier, D. Louer, G. Férey, *J. Am. Chem. Soc.*, 2002, **124**, 13519-13526.

35 C. Serre, S. Bourrelly, A. Vimont, N.A. Ramsahye, G. Maurin, P.L. Llewellyn, M. Daturi, Y. Filinchuk, O. Leynaud, P. Barnes, G. Férey, *Adv. Mater.*, 2007, **19**, 2246-2251.

36 P.L. Llewellyn, P. Horcajada, G. Maurin, T. Devic, N. Rosenbach, S. Bourrelly, C. Serre, D. Vincent, S. Loera-Serna, Y. Filinchuk, G. Férey, *J. Am. Chem. Soc.*, 2009, **131**, 13002-13008.

37 T.K. Trung, P. Trens, N. Tranchoux, S. Bourrelly, P.L. Llewellyn, S. Loera-Serna, C. Serre, T. Loiseau, F. Fajula, G. Ferey, *J.Am.Chem.Soc.*, 2008, **130**, 16926-16932.

38 A. Boutin, F.-X. Coudert, M.-A. Springuel-Huet, A.V. Neimark, G. Ferey, A.H. Fuchs, *J. Phys. Chem. C*, 2010, **114**, 22237-22244.

39 N. Klein, C. Herzog, M. Sabo, I. Senkovska, J. Getzschmann, S. Paasch, M.R. Lohe, E. Brunner, S. Kaskel, *Phys. Chem. Chem. Phys.*, 2010, **12**, 11778-11784.

40 A. Boutin, S. Couck, F.-X. Coudert, P. Serra-Crespo, J. Gascon, F. Kapteijn, A.H. Fuchs, J.F.M. Denayer, *Micropor. Mesopor. Mater.*, 2011, **140**, 108-113.

41 F.-X. Coudert, M. Jeffros, A.H. Fuchs, A. Boutin, C. Mellot-Draznieks, *J. Am. Chem. Soc.*, 2008, **130**, 14294-14302.

42 J. Lincke, D. Lässig, J. Möllmer, C. Reichenbach, A. Puls, A. Möller, R. Gläser, G. Kalies, R. Staudt, H. Krautscheid, *Micropor. Mesopor. Mater.*, 2011, **142**, 62-69.

43 C. Reichenbach, G. Kalies, J. Lincke, D. Lässig, H. Krautscheid, J. Moellmer, M. Thommes, *Micropor. Mesopor. Mater.*, 2011, **150**, 592-600.

44 D. Lässig, J. Lincke, H. Krautscheid, *Tetrahedron Lett.*, 2010, **51**, 653–656.

45 A. L. Platon, *J. Spek, Appl. Cryst.*, 2003, **36**, 7–13.

46 J. U. Keller, R. Staudt, *Gas Adsorption Equilibria - Experimental Methods and Adsorption Isotherms*, Springer, New York, USA, 2004.

47 W. Wagner, Ruhr-Universität Bochum, program FLUIDCAL; http://www.thermo.ruhr-uni-bochum.de/de/prof-w-wagner/software/fluidcal.html (10.10.2013).

48 K.S.W. Sing, D.H. Everett, R.A.W. Haul, L. Mouscou, R.A. Pierotti, J. Rouquerol, T. Siemieniewska, *Pure Appl. Chem.*, 1985, **57**, 603–619.

49 A. Boutin, M.-A. Springuel-Huet, A. Nossov, A. Gedeon, T. Loiseau, C. Volkringer, G. Ferey, F.-X. Coudert, A.H. Fuchs, *Angew. Chem. Int. Ed.*, 2009, **48**, 8314-8317.

50 M. Hartmann, S. Kunz, D. Himsl, O. Tangermann, S. Ernst, A. Wagener, *Langmuir* , 2008, **24**, 8634-8642.

51 N. Klein, I. Senkovska, K. Gedrich, U. Stoeck, A. Henschel, U. Mueller, S. Kaskel, *Angew. Chem. Int. Ed.*, 2009, **48**, 9954 –9957.

52 N. Klein, C. Herzog, M. Sabo, I. Senkovska, J. Getzschmann, S. Paasch, M.R. Lohe, E. Brunner, S. Kaskel, *Phys. Chem. Chem. Phys.*, 2010, **12**, 11778-11784.

53 K. Gedrich, I. Senkovska, N. Klein, U. Stoeck, A. Henschel, M.R. Lohe, I.A. Baburin, U. Mueller, S. Kaskel, *Angew. Chem.*, 2010, **122**, 8667 –8670.

54 R. Grünker, I. Senkovska, R. Biedermann, N. Klein, M.R. Lohe, P. Müller, S. Kaskel, *Chem. Commun.*, 2011, **47**, 490–492.

55 W. Zhu, J.C. Groen, F. Kapteijn, J.A. Moulijn, Langmuir 2004, **20**, 5277-5284.

56 B.B. Saha, A. Chakraborty, S. Koyama, S.-H. Yoon, I. Mochida, M. Kumja, C. Yap, K.C. Ng, *Int. J. Heat Mass Transfer*, 2008 **51**, 1582-1589.

57 A. Möller, A.P. Guimaraes, R. Gläser, R. Staudt, *Micropor. Mesopor. Mater.*, 2009, **125**, 23-29.

58 M.-G. Olivier, K. Berlier, R. Jadot, *J. Chem. Eng. Data*, 1994, **39**, 770-773.

59 N. Lamia, M. Jorge, M.A. Granato, F.A. Almeida Paz, H. Chevreau, A.E. Rodrigues, *Chem. Eng. Sciene, 2009*, **6**, 3240-3259.

60 S.H. Hyun, R.P. Danner, *J. Chem. Eng. Data*, 1982, **27**, 196-200.

61 L. Gurvich, *J. Phys. Chem. Soc. Russ.*, 1915, **47**, 805–827.

62 S. Lowell, J. Shields, M.A. Thomas, M. Thommes, *Characterization of Porous Solids and Powders: Surface Area, Pore Size and Density*, Springer, Dordrecht, 2004.

63 D.D. Do, *Adsorption Analysis: Equilibria and Kinetics in Series on Chemical engineering Vol.2*, Imperial College Press, London, 1998.

64 I. Langmuir, *J. Am. Chem. Soc.*, 1918, **40**, 1361.

65 D. Farrusseng, C. Daniel, C. Gaudillere, U. Ravon, Y. Schuurman, C. Mirodates, D. Dubbeldam, H. Frost, R. Snurr, *Langmuir*, 2009, **25**, 7383-7388.

66 P.L. Llewellyn, G. Maurin, T. Devic, S. Loera-Serna, N. Rosenbach, C. Serre, S. Bourrelly, P. Horcajada, Y. Filinchuk, G. Férey, *J. Am. Chem. Soc.*, 2008, **130**, 12808-12814.

67 S. Couck, T. Rèmy, G.V. Baron, J. Gascon, F. Kapteijn, J.F.M. Denayer, *Phys. Chem. Chem. Phys.*, 2010, **12**, 9413-9418.

Electronic Supplementary Information (ESI)

Structural Flexibility of a Copper-Based Metal Organic Framework: Adsorption of C_4-hydrocarbons and *in situ* XRD

Marcus Lange,[a] Merten Kobalz,[b] Jens Bergmann,[b] Daniel Lässig,[b] Jörg Lincke,[b] Jens Möllmer,[a] Andreas Möller,[a] Jörg Hofmann,[a] Harald Krautscheid,[b] Reiner Staudt[c] and Roger Gläser*[a]

[a] *Institut für Nichtklassische Chemie e.V., Permoserstraße 15, D-04318 Leipzig, Germany*

[b] *Universität Leipzig, Fakultät für Chemie und Mineralogie, Johannisallee 29, D-04103 Leipzig, Germany*

[c] *University of Applied Sciences Offenburg, Badstraße 24, D-77652 Offenburg, Germany;*

Tables

Table SI 1 Pore volumes of $^{3}_{\infty}[Cu_4(\mu_4\text{-}O)(\mu_2\text{-}OH)_2(Me_2trz\textit{p}ba)_4]$ (**1**) for N2/ 77 K and CO2 /298 K sorption.

	After 1st pore filling		**Saturation**		**Ref.**
	p/p$_0$	**V$_{pore}$ / cm^3 g^{-1}**	**p/p$_0$**	**V$_{pore}$ / cm^3 g^{-1}**	
N_2 at 77 K	0.001	0.16	0.90	0.58	1
CO_2 at 298 K	0.050	0.13	0.90	0.53	
N_2 at 77 K	0.030	0.16	0.60	0.59	this study
CO_2 at 298 K	0.001	0.14	0.68	0.54	

Table SI 2 Physical properties including critical temperature (T_C), critical pressure (p_C), critical density (ρ_C), boiling point (T_b) and density at boiling point (ρ_b) of carbon dioxide, nitrogen and C_4-hydrocarbons.

	CO_2	**N_2**	***n*-butane**	**isobutane**	**1-butene**	**isobutene**
T_C / K	304.15	126.25	425.15	408.13	419.65	417.85
p_C / MPa	7.38	3.40	3.80	3.65	4.02	4.00
ρ_C / (g cm^{-3})	0.468	0.314	0.228	0.221	0.234	0.234
T_b / K	-	77.15	272.65	261.45	266.95	266.05
ρ_b / (g cm^{-3})	-	0.809	0.601	0.594	0.626	0.626

Table SI 3 Parameters for Langmuir-Fits for different temperatures with fixed N_{max} (283 K).

	283 K	**298 K**	**313 K**	**328 K**	**343 K**
	***n*-butane on 1 with fixed N_{max}**				
N_{max} / mmol g^{-1}	0.980				
b / kPa^{-1}	53.981	16.867	6.307	2.759	1.282
R^2	0.99954	0.99915	0.99927	0.99899	0.99902
	isobutane on 1 with fixed N_{max}				
N_{max} / mmol g^{-1}	0.858				
b / kPa^{-1}	54.111	18.294	6.585	2.887	1.428
R^2	0.99960	0.99985	0.99965	0.99957	0.99982
	1-butene on 1 with fixed N_{max}				
N_{max} / mmol g^{-1}	1.501				
b / kPa^{-1}	6.380	20.449	2.214	0.976	0.562
R^2	0.98974	0.98993	0.99116	0.98607	0.98716
	isobutene on 1 with fixed N_{max}				
N_{max} / mmol g^{-1}	2.124				
b / kPa^{-1}	7.415	3.267	1.377	0.598	0.305
R^2	0.99279	0.99904	0.99319	0.99589	0.98845

Figures

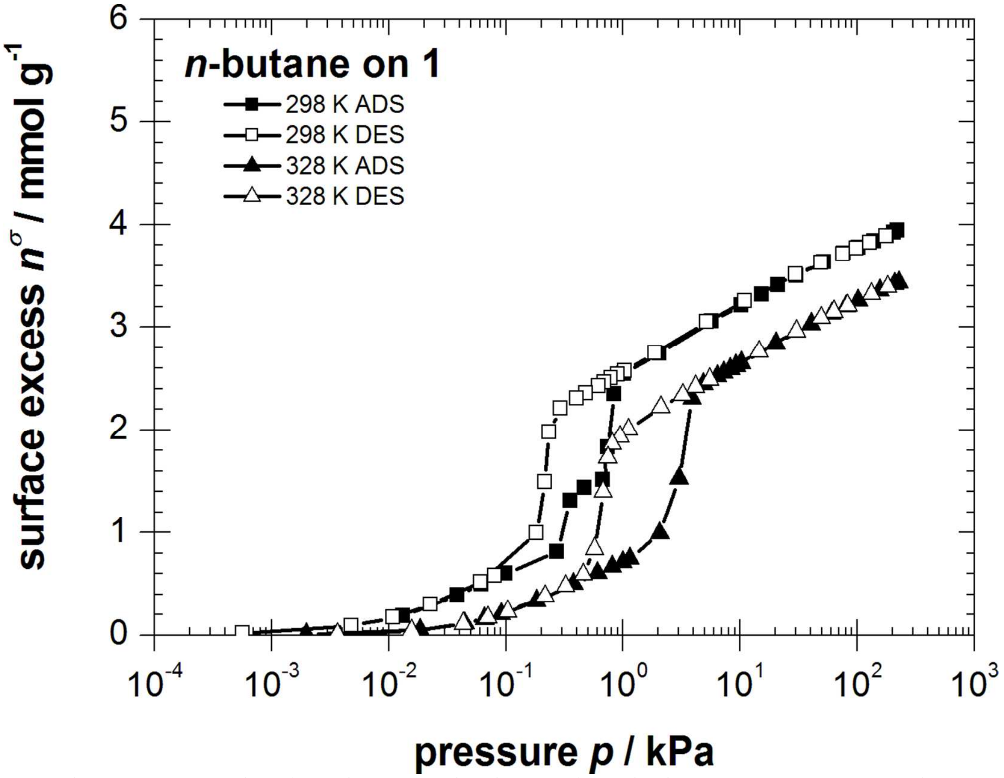

Fig. SI 1 Surface excess as a function of pressure for the sorption of *n*-butane on **1** at 298 K and 328 K (ADS: adsorption, DES: desorption).

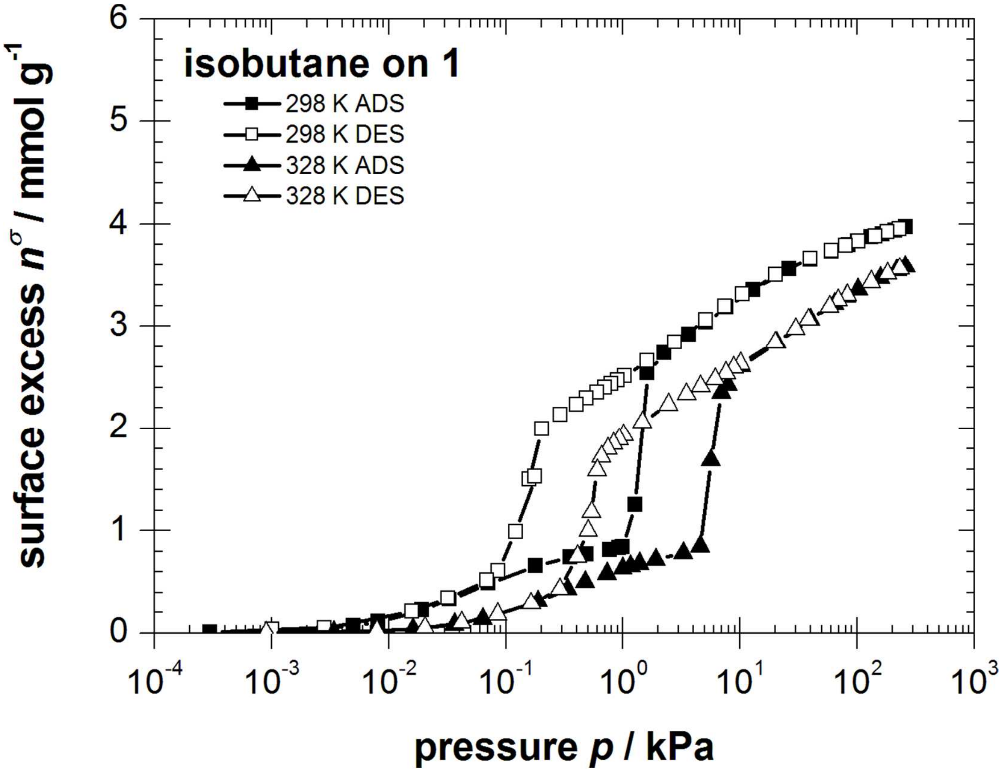

Fig. SI 2 Surface excess as a function of pressure for the sorption of isobutane on **1** at 298 K and 328 K (ADS: adsorption, DES: desorption).

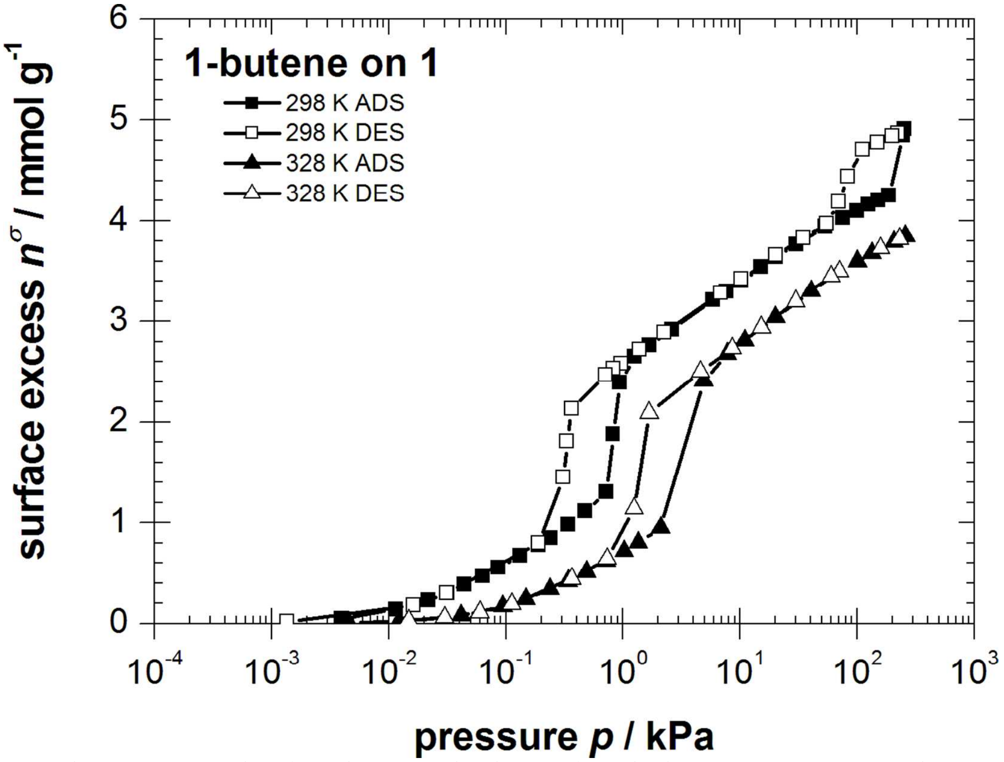

Fig. SI 3 Surface excess as a function of pressure for the sorption of 1-butene on **1** at 298 K and 328 K (ADS: adsorption, DES: desorption).

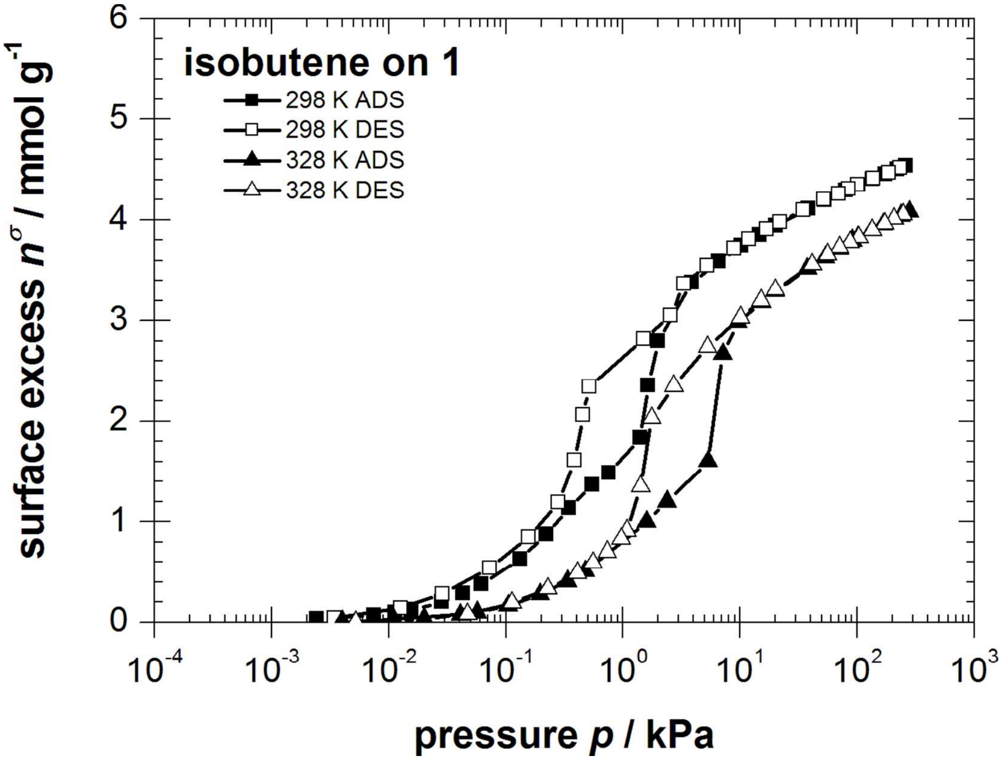

Fig. SI 4 Surface excess as a function of pressure for the sorption of isobutene on **1** at 298 K and 328 K (ADS: adsorption, DES: desorption).

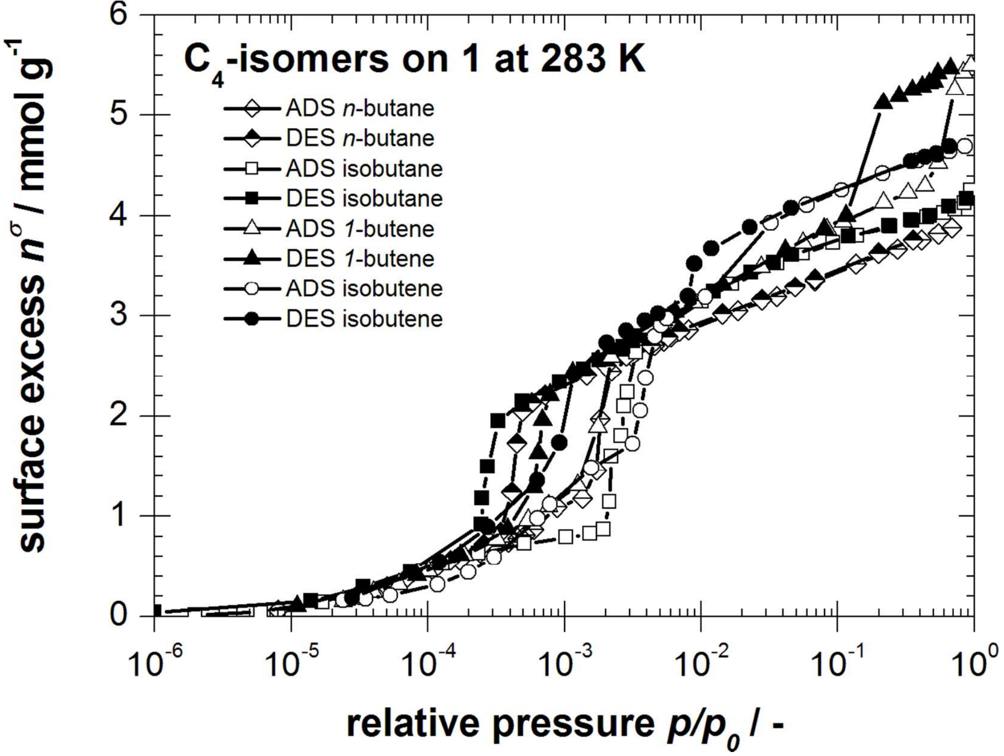

Fig. SI 5 Adsorption (ADS, open symbols) and desorption (DES, closed symbols) isotherms of investigated C_4-hydrocarbons, including *n*-butane (diamonds), isobutane (squares), 1-butene (triangles) and isobutene (circles) on **1** at 283 K up to relative pressures $p/p_0 = 1$.

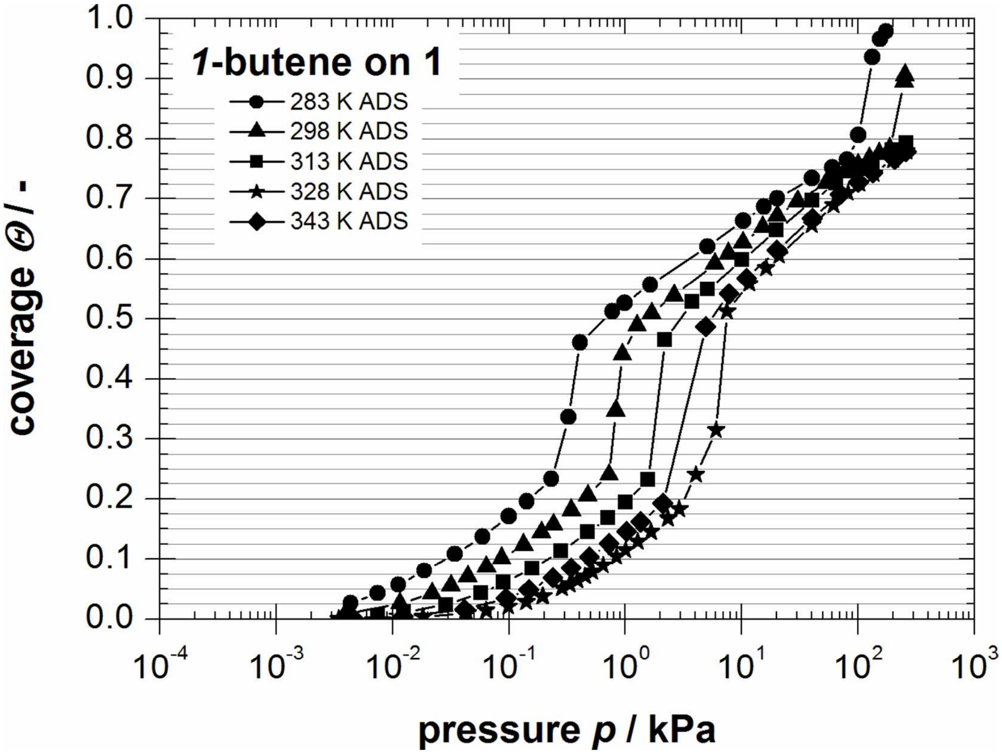

Fig. SI 6 Coverage of 1-butene on **1** as a function of Pressures for different temperatures. Intermediate values were interpolated.

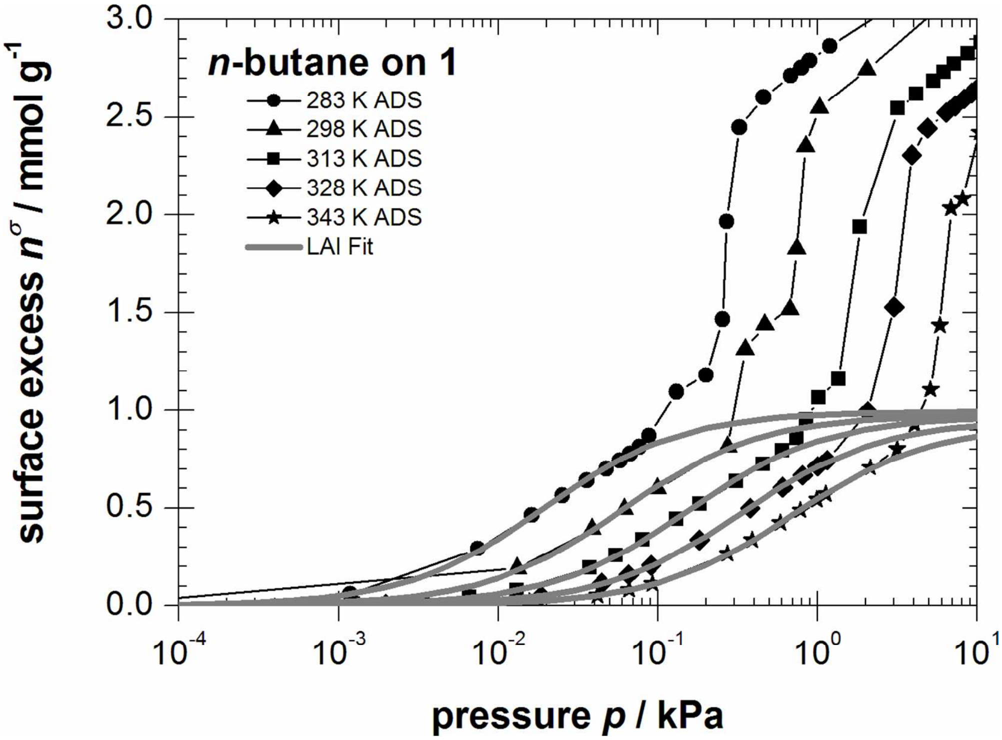

Fig. SI 7 Adsorption isotherms of *n*-butane on **1** at 283 K (circles), 298 K (triangles), 313 K (squares), 328 K (diamonds) and 343 K (stars) with Langmuir-Fits (strong grey lines) for pore filling in low pressure region – black lines are to guide the eyes.

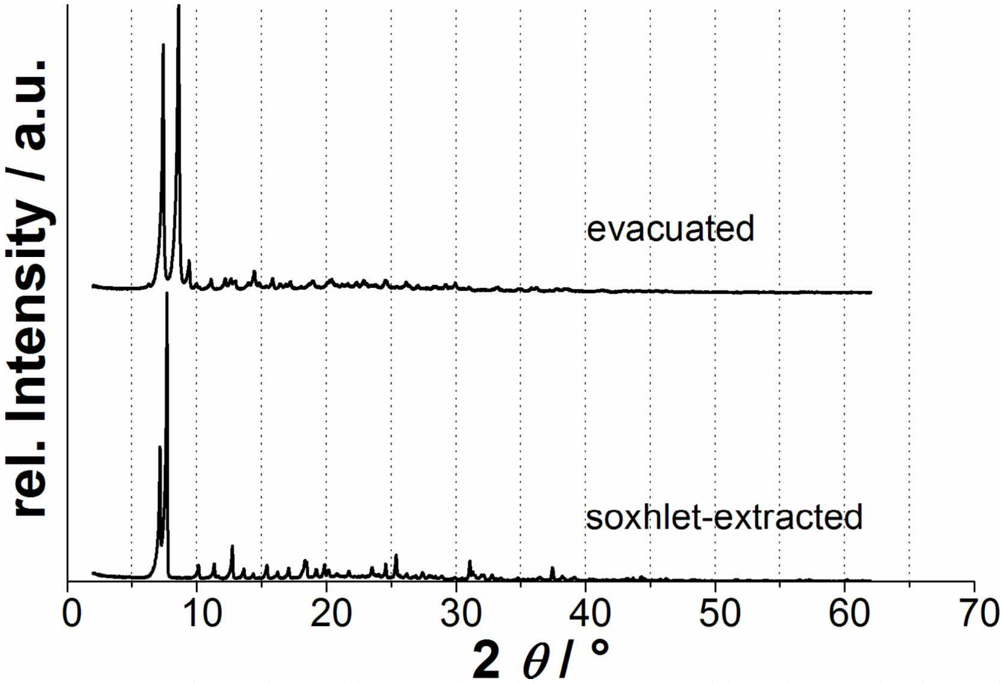

Fig. SI 8 XRD pattern for **1** after soxhlet-extraction with MeOH (opened by solvent molecules) and under vacuum.

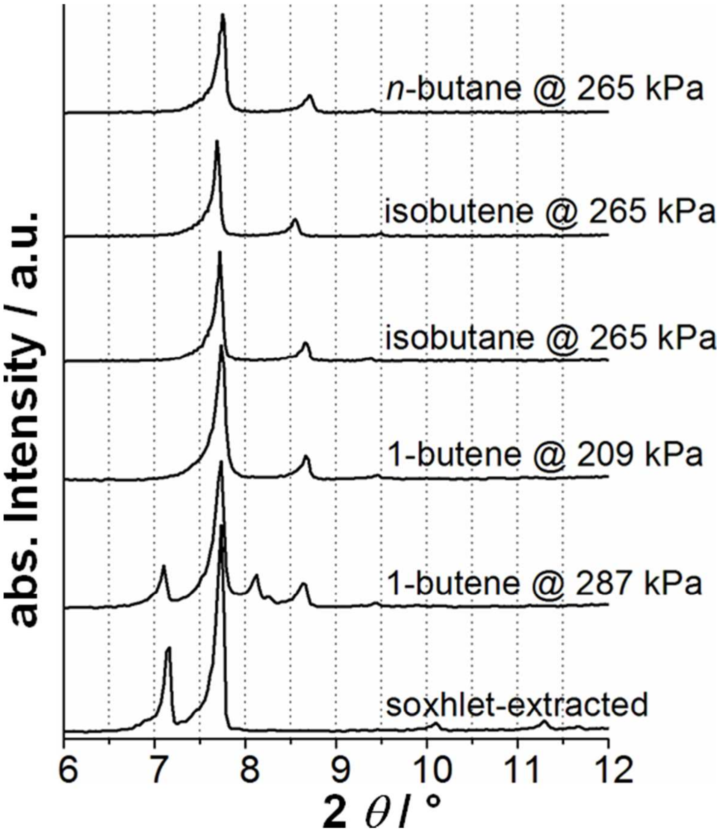

Fig. SI 9 XRD patterns of **1** filled with solvent molecules (after MeOH soxhlet-extraction) and with different sorptives at 298 K and comparable pressures.

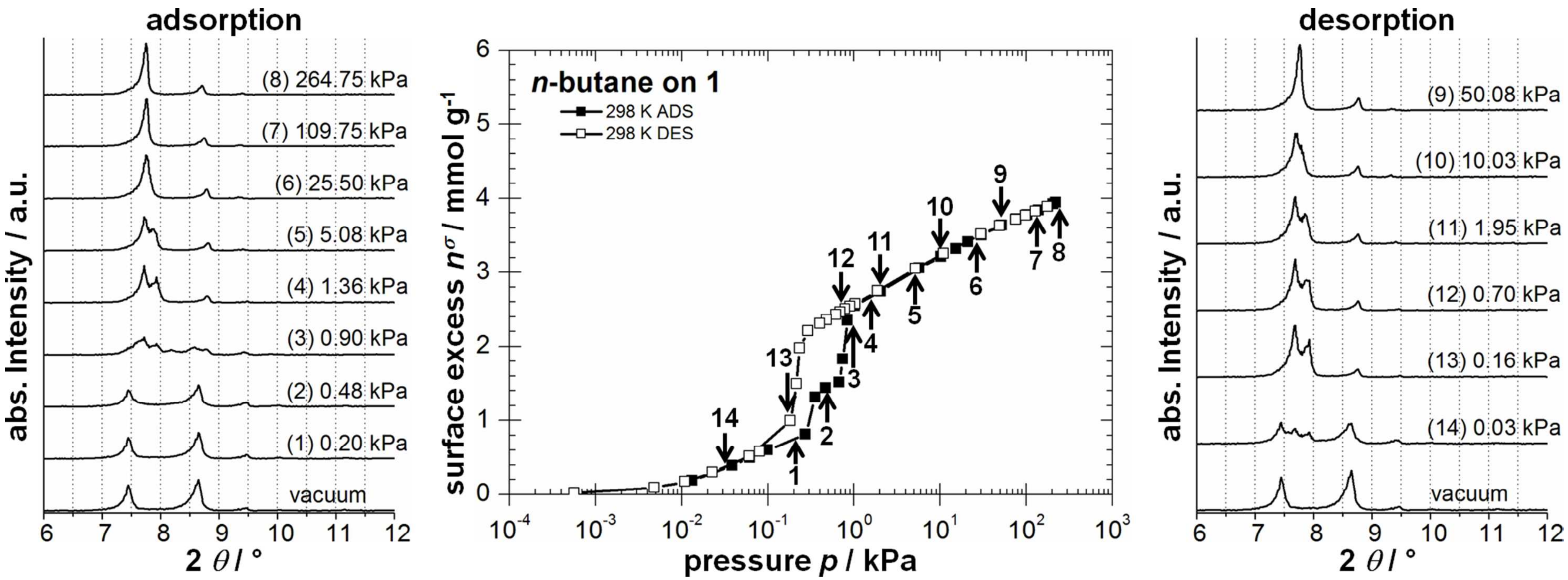

Fig. SI 10 Adsorption (closed symbols) and desorption (open symbols) isotherm of *n*-butane on **1** (center) at 298 K and XRD patterns of **1** at different pressures for adsorption (left) and desorption (right). The respective points on the sorption isotherms at which the XRD patterns were recorded are labelled as 1 – 14. The gate-opening is observed at about 1 kPa (point 3).

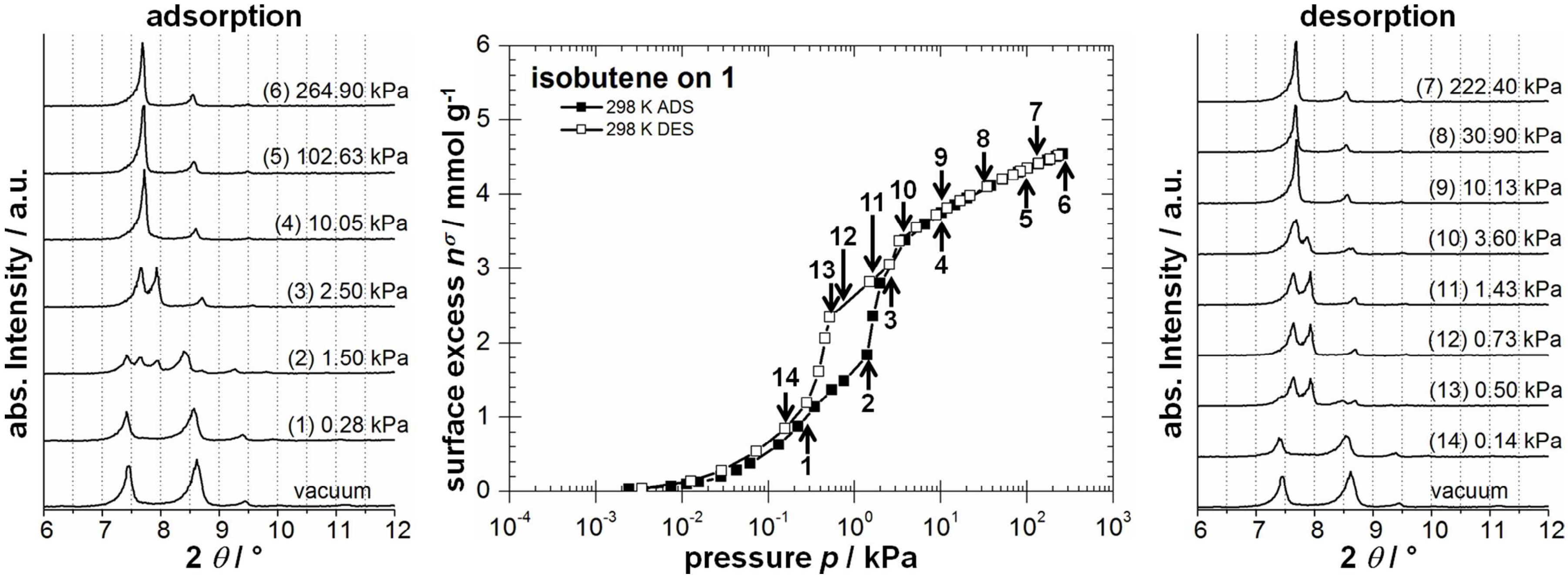

Fig. SI 11 Adsorption (closed symbols) and desorption (open symbols) isotherm of isobutene on **1** (center) at 298 K and XRD patterns of **1** at different pressures for adsorption (left) and desorption (right). The respective points on the sorption isotherms at which the XRD patterns were recorded are labelled as 1 – 14.The gate-opening is observed at about 1.5 kPa (point 2).

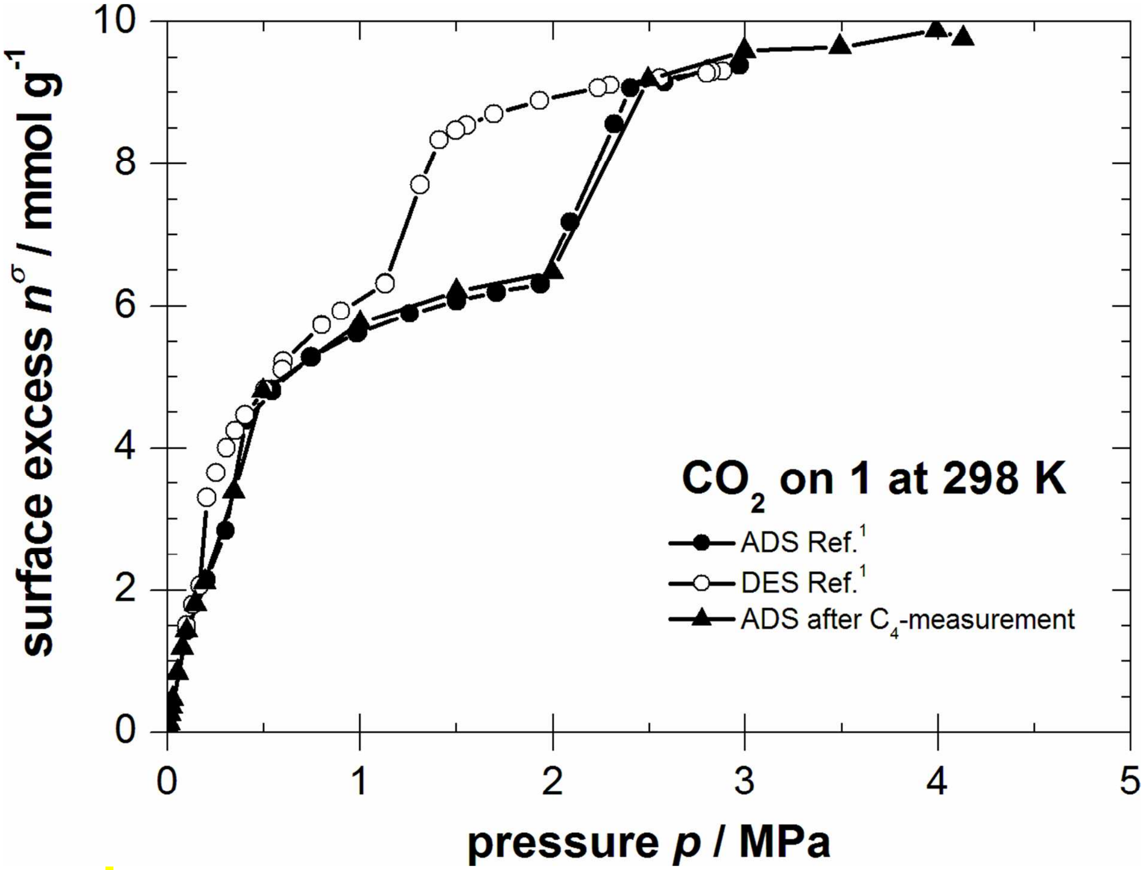

Fig. SI 12 Adsorption and desorption isotherms of carbon dioxide on **1** at 298 K after C_4-hydrocarbon sorption experiments compared to published data byRef.[1]

References

1 J. Lincke, D. Lässig, J. Möllmer, C. Reichenbach, A. Puls, A. Möller, R. Gläser, G. Kalies, R. Staudt, H. Krautscheid, *Micropor. Mesopor. Mater.*, 2011, **142**, 62-69.

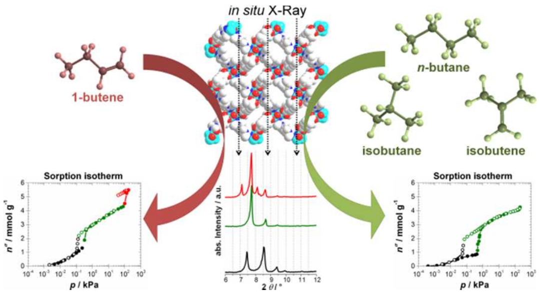

Structural transitions of a flexible Cu-MOF are observed by pressure-dependent *in situ* XRD with C_4-hydrocarbons whereby only 1-butene sorption shows two transformations.

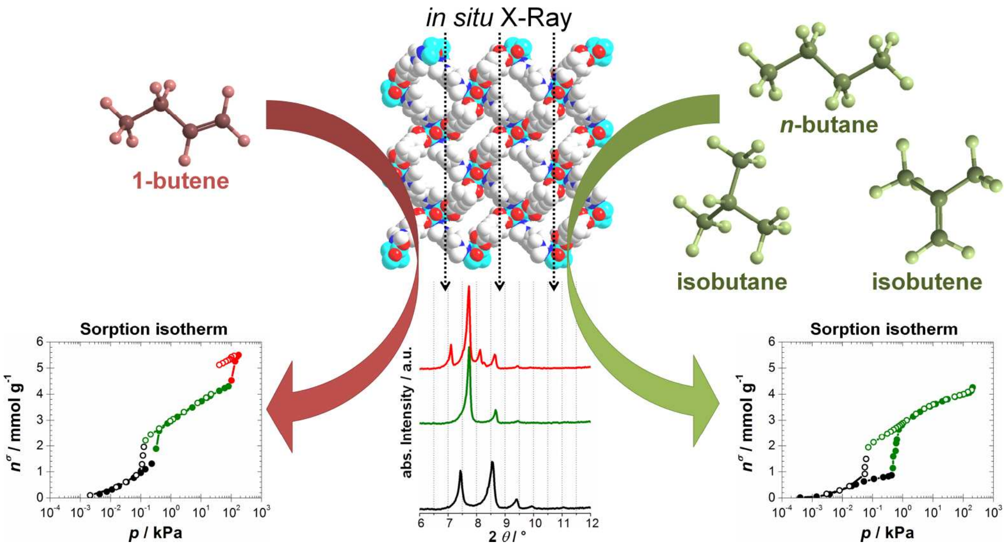

232x124mm (300 x 300 DPI)

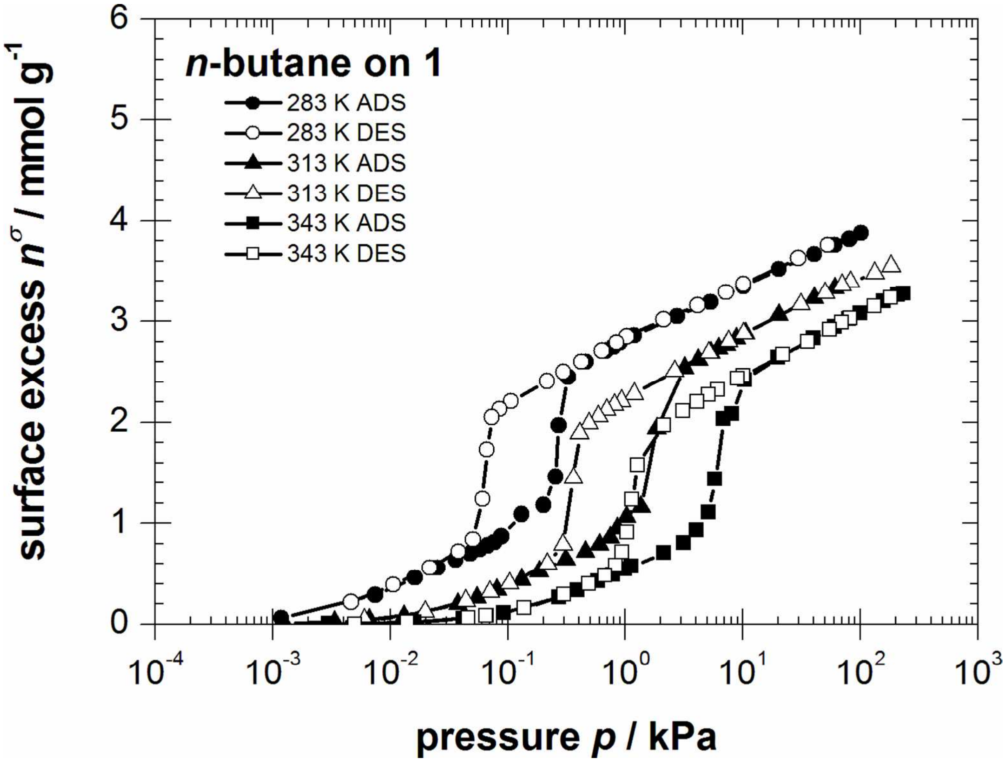

238x180mm (150 x 150 DPI)

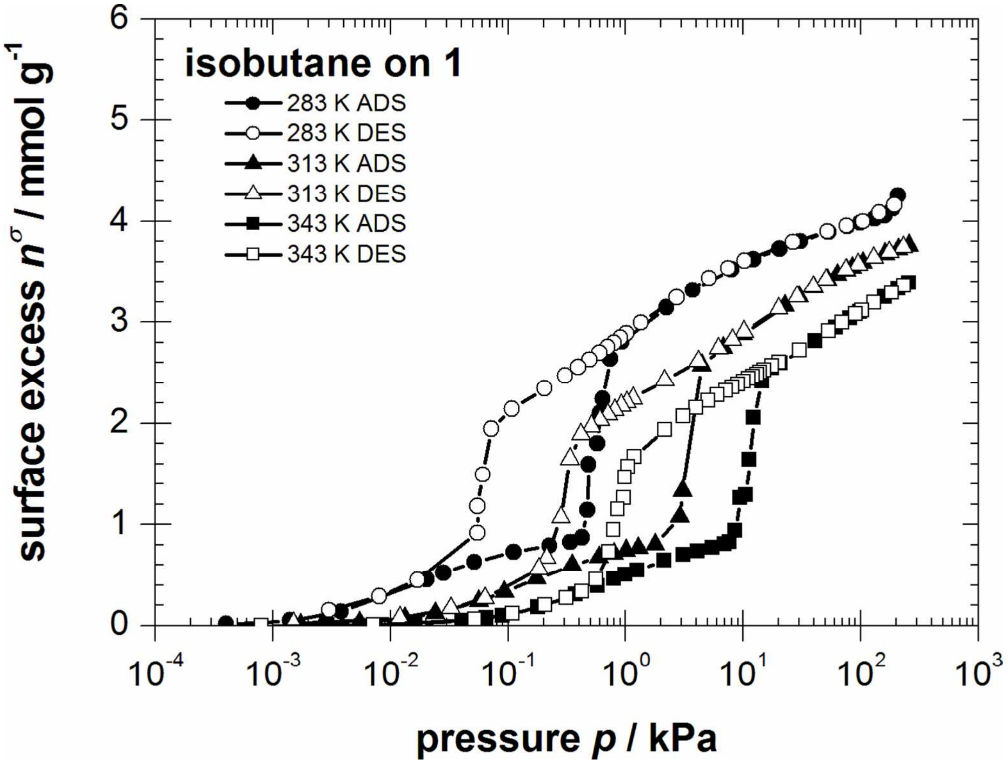

238x180mm (150 x 150 DPI)

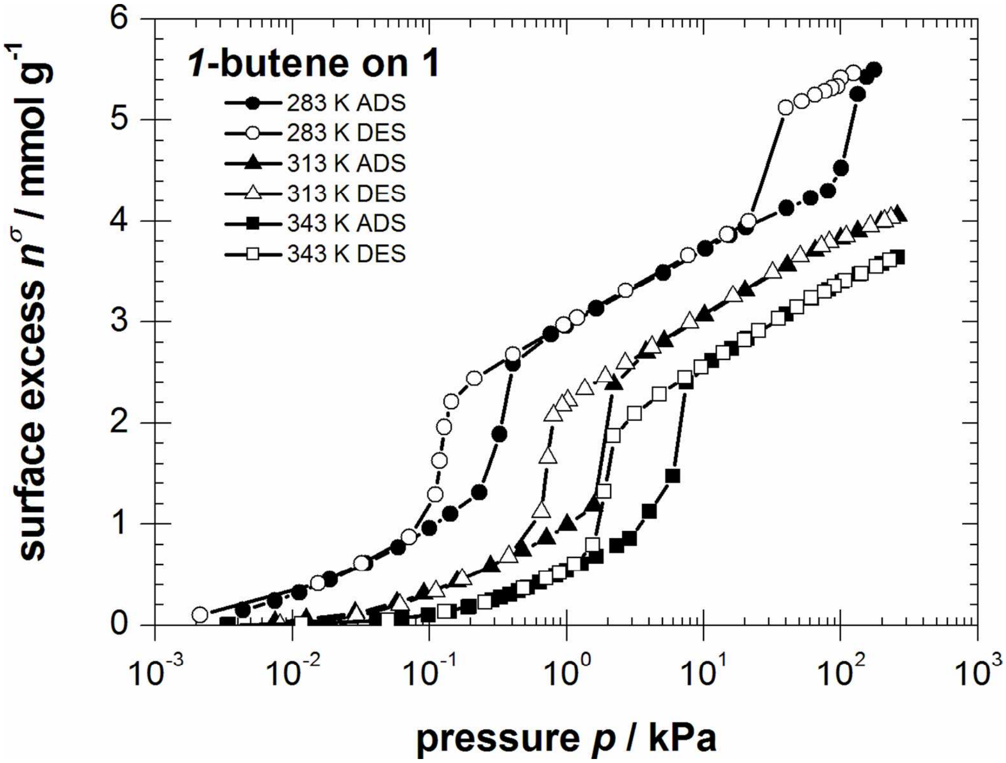

238x180mm (150 x 150 DPI)

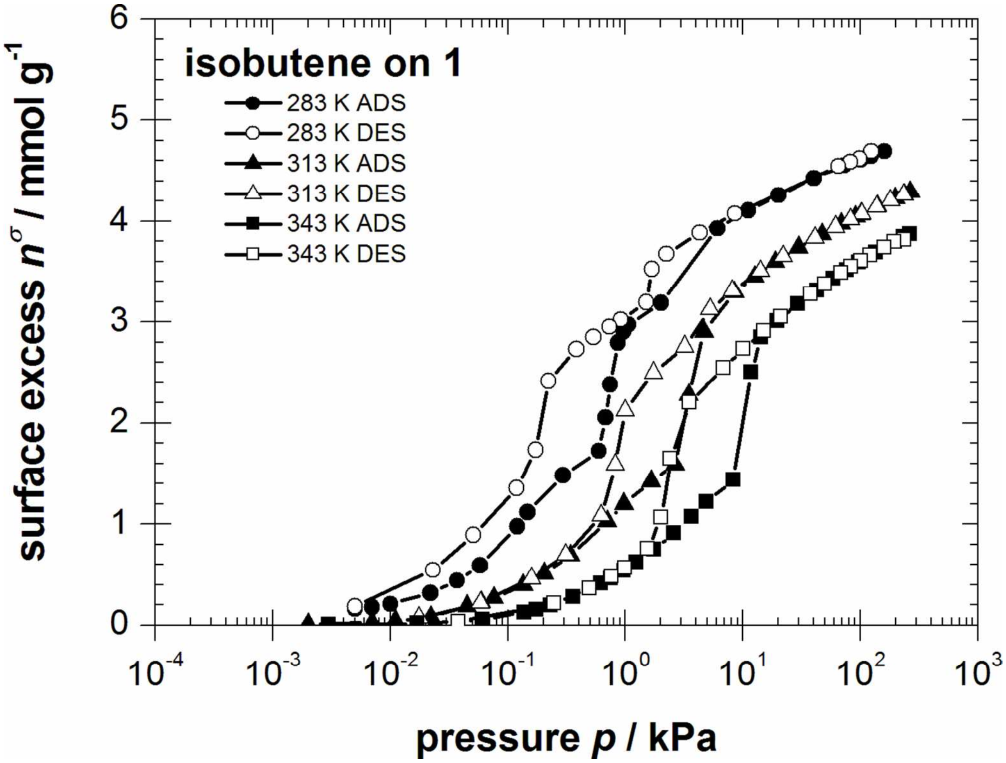

238x180mm (150 x 150 DPI)

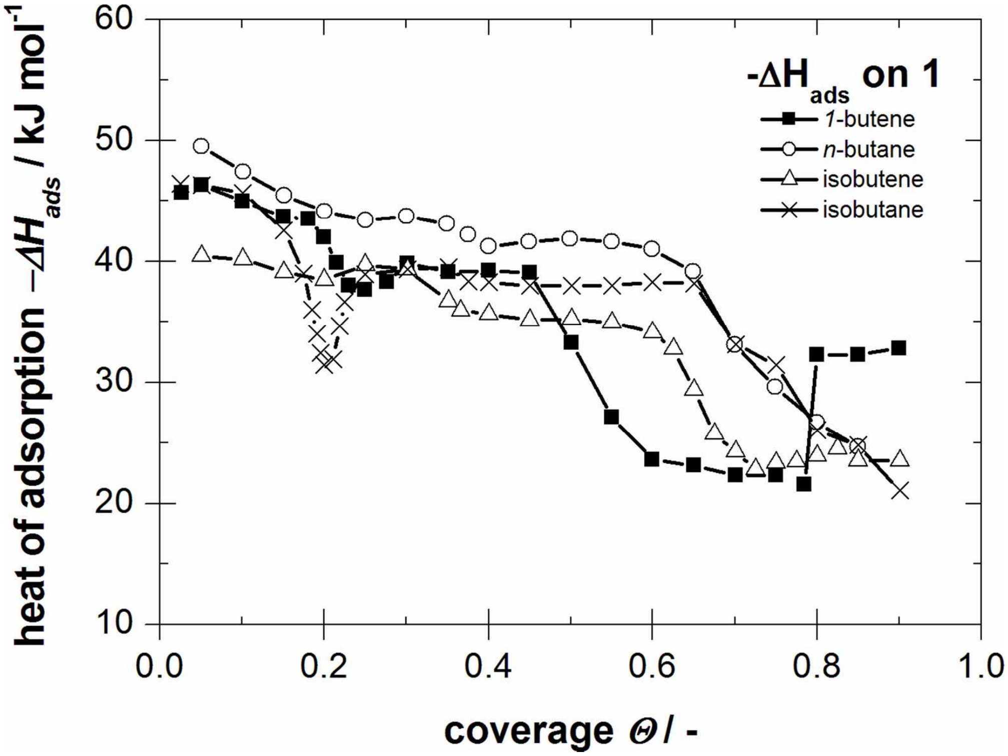

239x178mm (150 x 150 DPI)

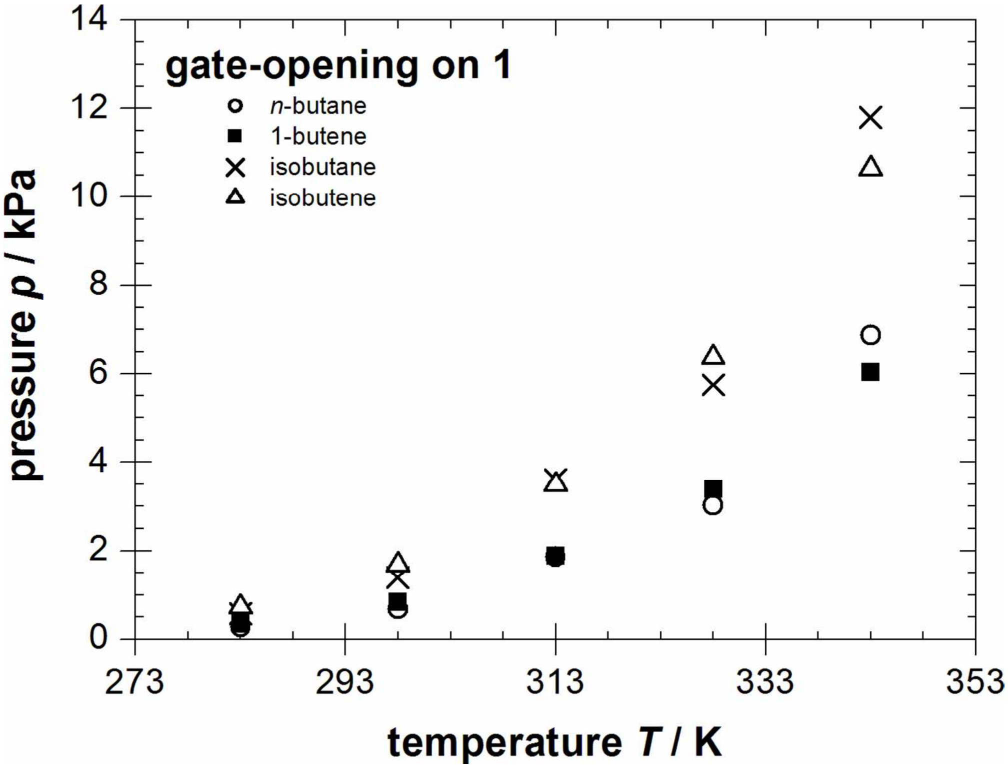

234x177mm (150 x 150 DPI)

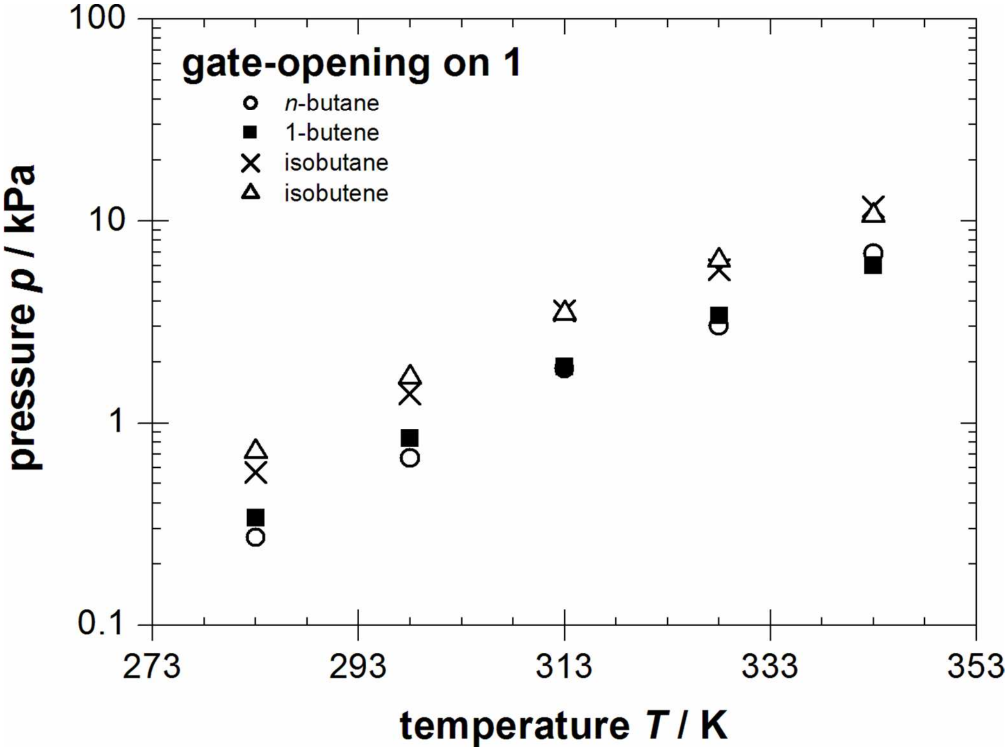

238x177mm (150 x 150 DPI)

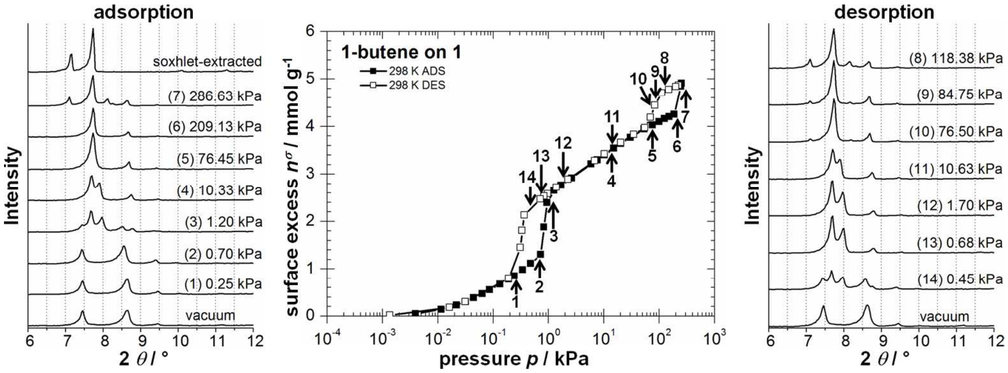
adsorption
Intensity
soxhlet-extracted
(7) 286.63 kPa
(6) 209.13 kPa
(5) 76.45 kPa
(4) 10.33 kPa
(3) 1.20 kPa
(2) 0.70 kPa
(1) 0.25 kPa
vacuum
6 7 8 9 10 11 12
2 θ / °
1-butene on 1
298 K ADS
298 K DES
surface excess n^{σ} / mmol g^{-1}
0 1 2 3 4 5 6
10^{-4} 10^{-3} 10^{-2} 10^{-1} 10^{0} 10^{1} 10^{2} 10^{3}
pressure p / kPa
1 2 3 4 5 6 7 8 9 10 11 12 13 14
desorption
Intensity
(8) 118.38 kPa
(9) 84.75 kPa
(10) 76.50 kPa
(11) 10.63 kPa
(12) 1.70 kPa
(13) 0.68 kPa
(14) 0.45 kPa
vacuum
6 7 8 9 10 11 12
2 θ / °

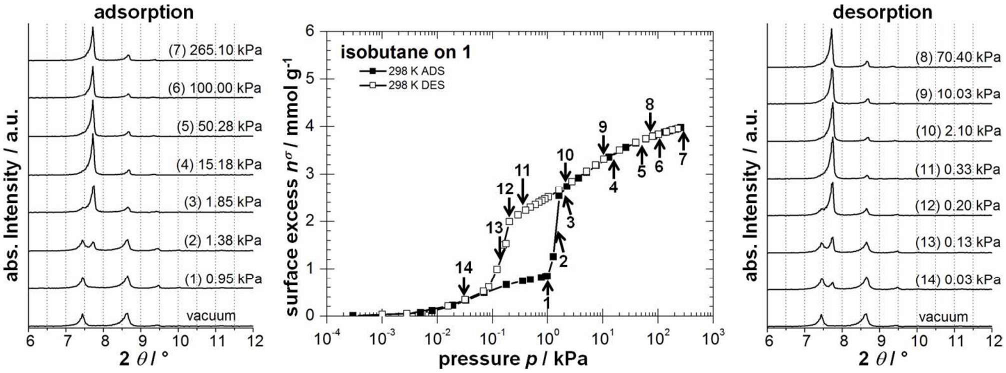
adsorption
abs. Intensity / a.u.
(7) 265.10 kPa
(6) 100.00 kPa
(5) 50.28 kPa
(4) 15.18 kPa
(3) 1.85 kPa
(2) 1.38 kPa
(1) 0.95 kPa
vacuum
6 7 8 9 10 11 12
2 θ / °
isobutane on 1
298 K ADS
298 K DES
surface excess n^σ / mmol g^{-1}
pressure p / kPa
10^{-4} 10^{-3} 10^{-2} 10^{-1} 10^{0} 10^{1} 10^{2} 10^{3}
0 1 2 3 4 5 6
1 2 3 4 5 6 7 8 9 10 11 12 13 14
desorption
(8) 70.40 kPa
(9) 10.03 kPa
(10) 2.10 kPa
(11) 0.33 kPa
(12) 0.20 kPa
(13) 0.13 kPa
(14) 0.03 kPa
vacuum
6 7 8 9 10 11 12
2 θ / °

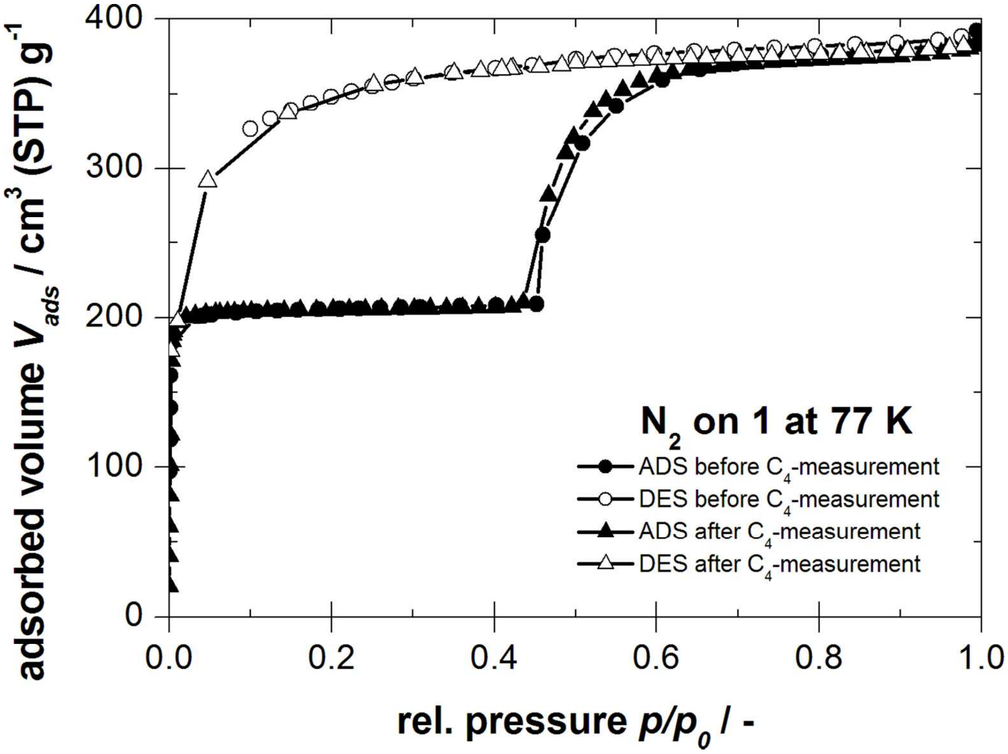
N$_2$ on 1 at 77 K
ADS before C$_4$-measurement
DES before C$_4$-measurement
ADS after C$_4$-measurement
DES after C$_4$-measurement
adsorbed volume V_{ads} / cm^3 (STP) g^{-1}
rel. pressure p/p_0 / -
0
100
200
300
400
0.0
0.2
0.4
0.6
0.8
1.0

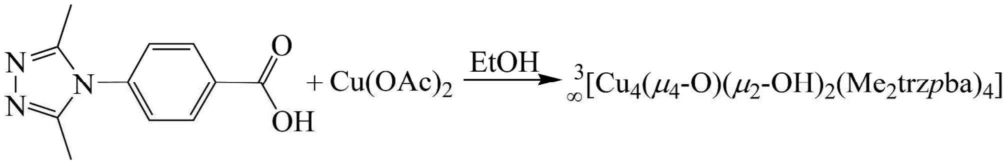

292x45mm (300 x 300 DPI)

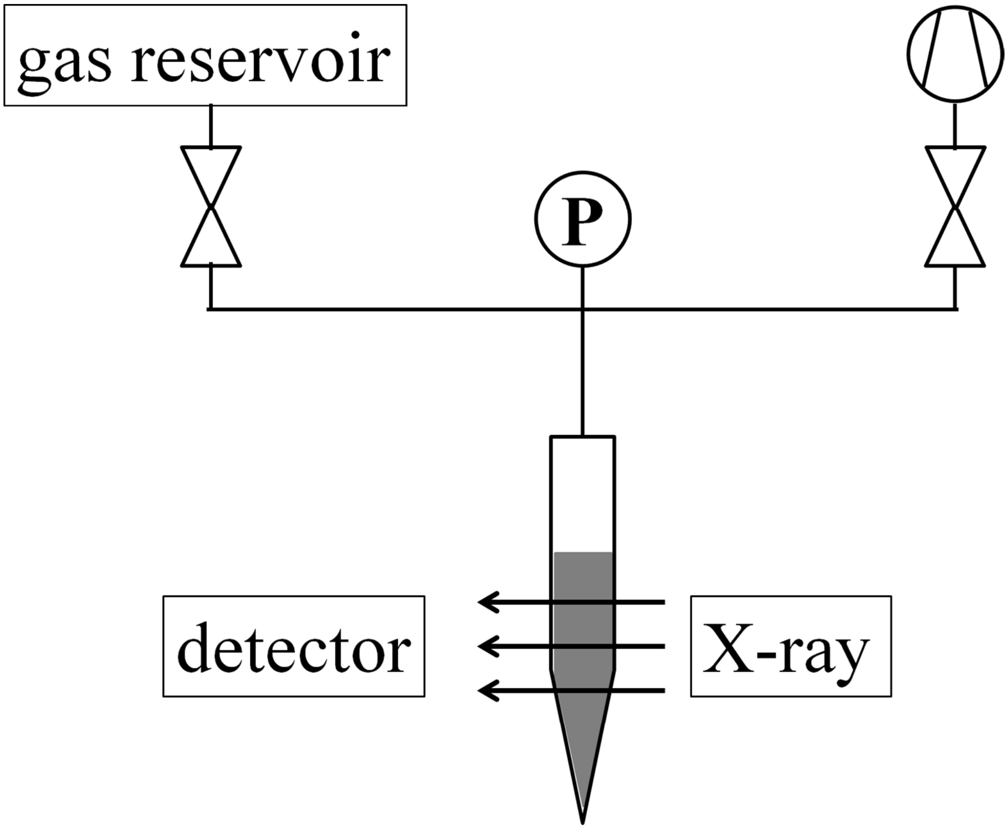
gas reservoir
P
detector
X-ray

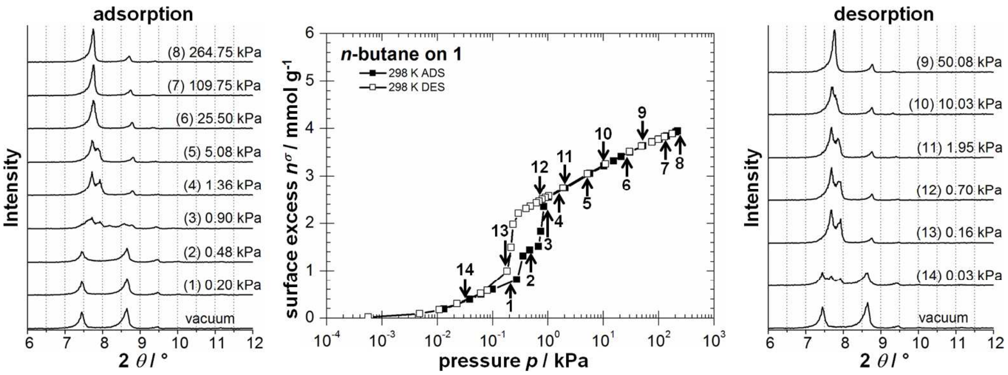
adsorption
Intensity
(8) 264.75 kPa
(7) 109.75 kPa
(6) 25.50 kPa
(5) 5.08 kPa
(4) 1.36 kPa
(3) 0.90 kPa
(2) 0.48 kPa
(1) 0.20 kPa
vacuum
6
7
8
9
10
11
12
2 θ / °
n-butane on 1
298 K ADS
298 K DES
surface excess n^{σ} / mmol g^{-1}
0
1
2
3
4
5
6
10^{-4}
10^{-3}
10^{-2}
10^{-1}
10^{0}
10^{1}
10^{2}
10^{3}
pressure *p* / kPa
1
2
3
4
5
6
7
8
9
10
11
12
13
14
desorption
Intensity
(9) 50.08 kPa
(10) 10.03 kPa
(11) 1.95 kPa
(12) 0.70 kPa
(13) 0.16 kPa
(14) 0.03 kPa
vacuum
6
7
8
9
10
11
12
2 θ / °

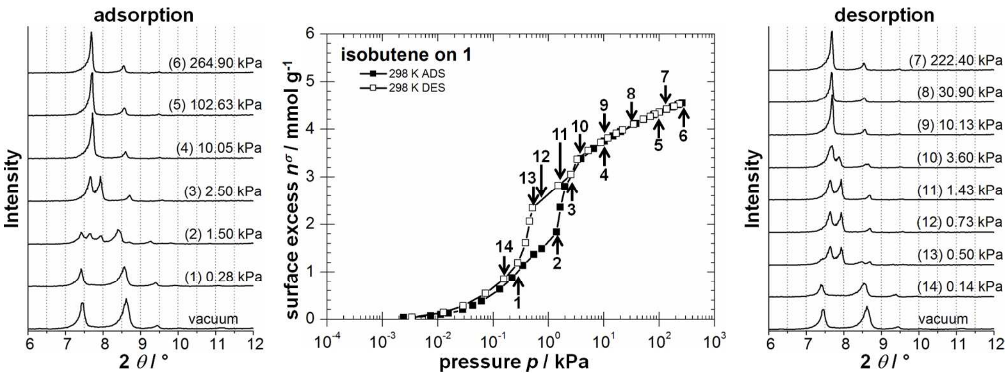
adsorption
Intensity
(6) 264.90 kPa
(5) 102.63 kPa
(4) 10.05 kPa
(3) 2.50 kPa
(2) 1.50 kPa
(1) 0.28 kPa
vacuum
6 7 8 9 10 11 12
2 θ / °
isobutene on 1
298 K ADS
298 K DES
surface excess n^σ / mmol g^{-1}
0 1 2 3 4 5 6
10^{-4} 10^{-3} 10^{-2} 10^{-1} 10^{0} 10^{1} 10^{2} 10^{3}
pressure p / kPa
1 2 3 4 5 6 7 8 9 10 11 12 13 14
desorption
Intensity
(7) 222.40 kPa
(8) 30.90 kPa
(9) 10.13 kPa
(10) 3.60 kPa
(11) 1.43 kPa
(12) 0.73 kPa
(13) 0.50 kPa
(14) 0.14 kPa
vacuum
6 7 8 9 10 11 12
2 θ / °

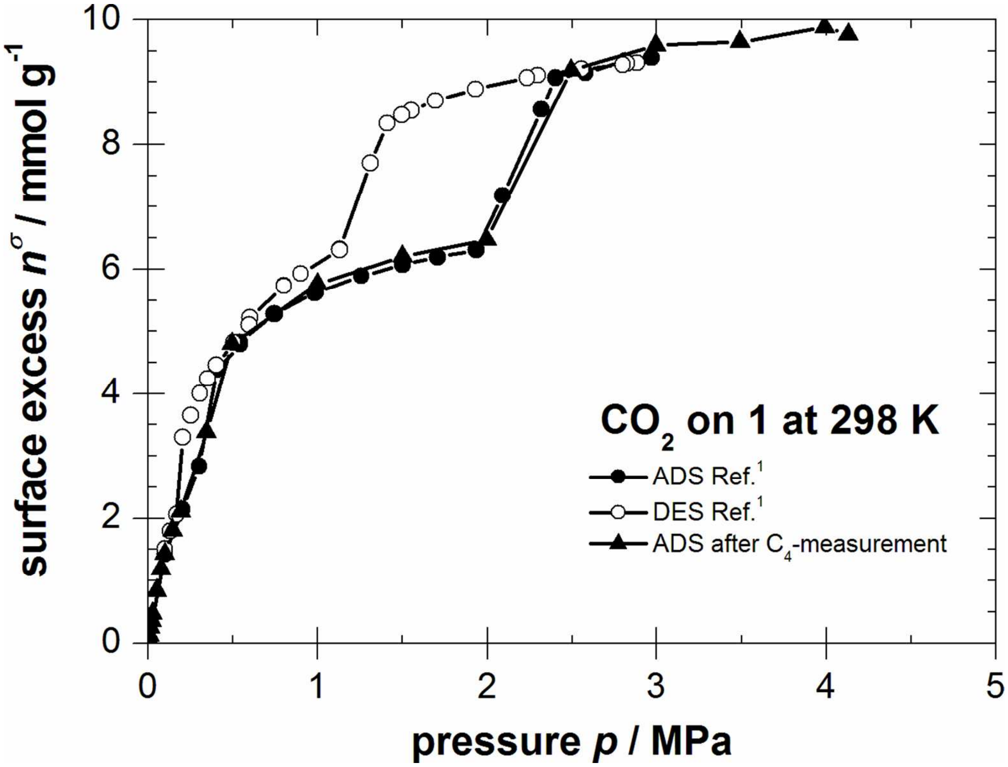

232x175mm (150 x 150 DPI)

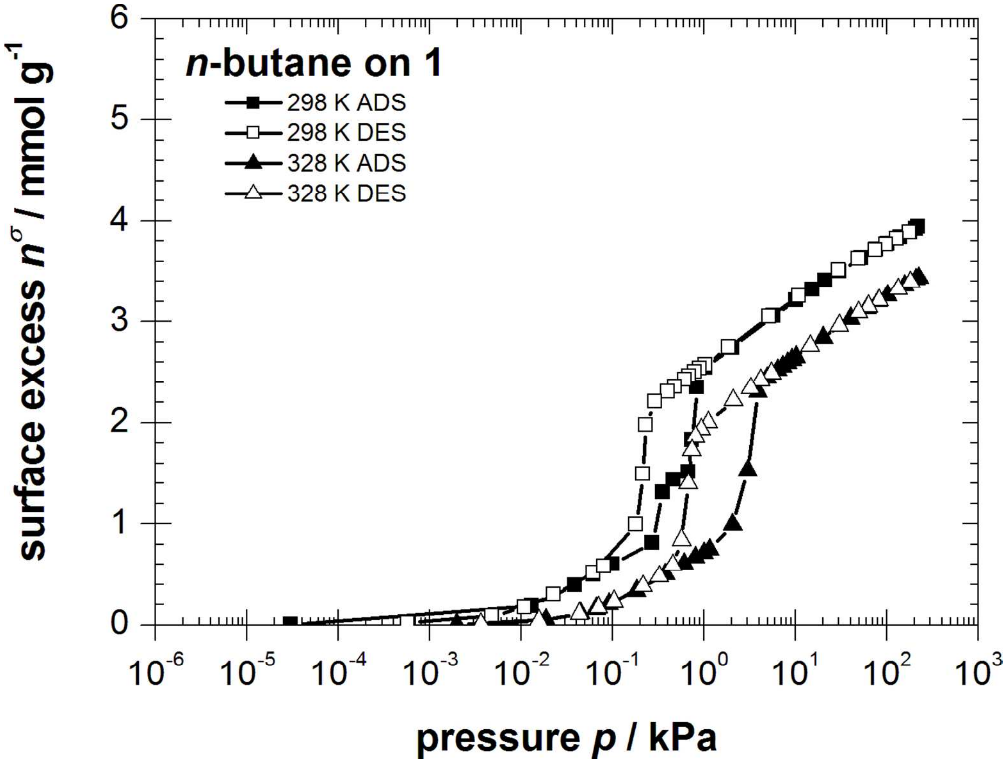
n-butane on 1
298 K ADS
298 K DES
328 K ADS
328 K DES
surface excess n^σ / mmol g^{-1}
pressure *p* / kPa
0
1
2
3
4
5
6
10^{-6}
10^{-5}
10^{-4}
10^{-3}
10^{-2}
10^{-1}
10^{0}
10^{1}
10^{2}
10^{3}

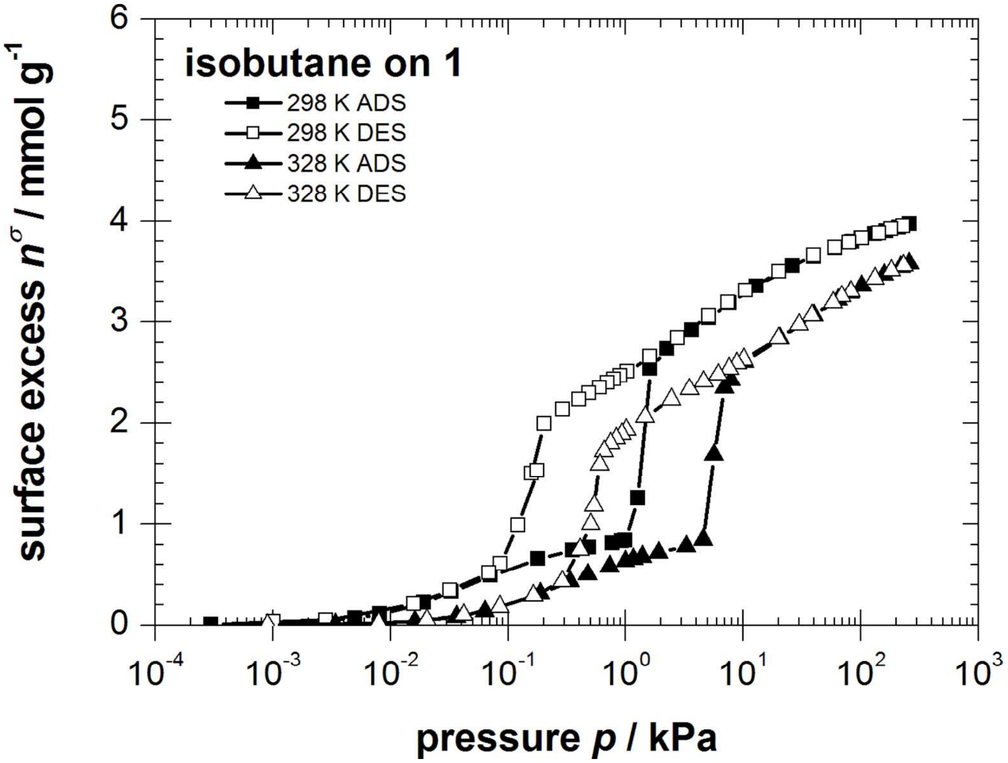
isobutane on 1
298 K ADS
298 K DES
328 K ADS
328 K DES
surface excess n^σ / mmol g^{-1}
pressure p / kPa
0
1
2
3
4
5
6
10^{-4}
10^{-3}
10^{-2}
10^{-1}
10^{0}
10^{1}
10^{2}
10^{3}

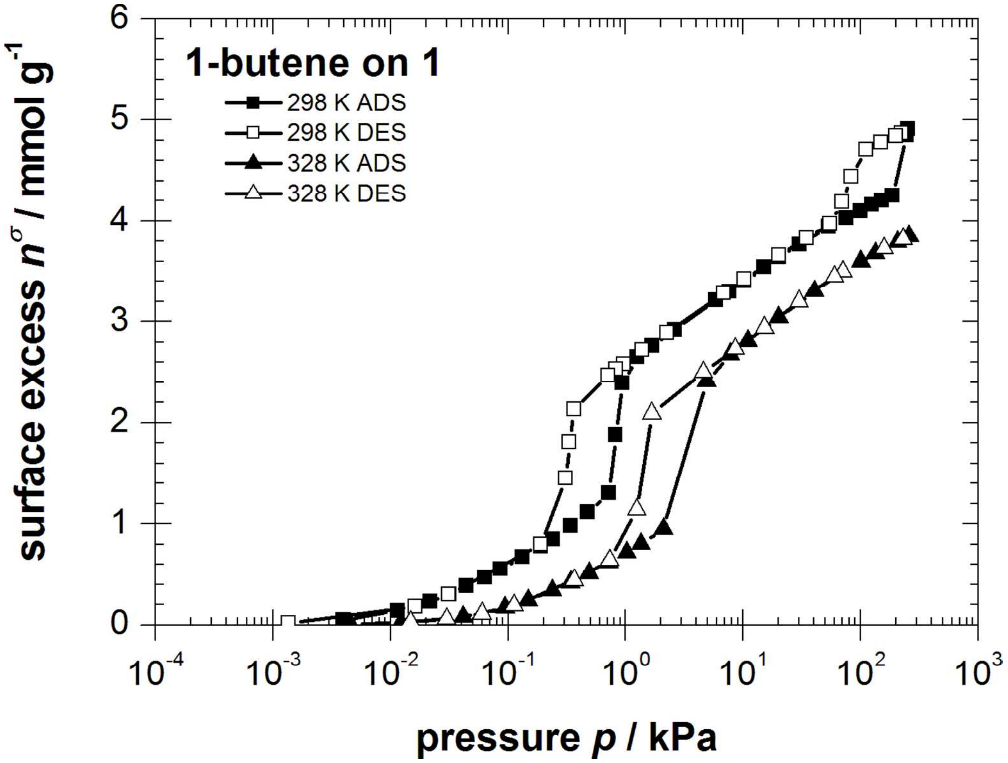
1-butene on 1
298 K ADS
298 K DES
328 K ADS
328 K DES
surface excess n^{σ} / mmol g^{-1}
0
1
2
3
4
5
6
10^{-4}
10^{-3}
10^{-2}
10^{-1}
10^{0}
10^{1}
10^{2}
10^{3}
pressure p / kPa

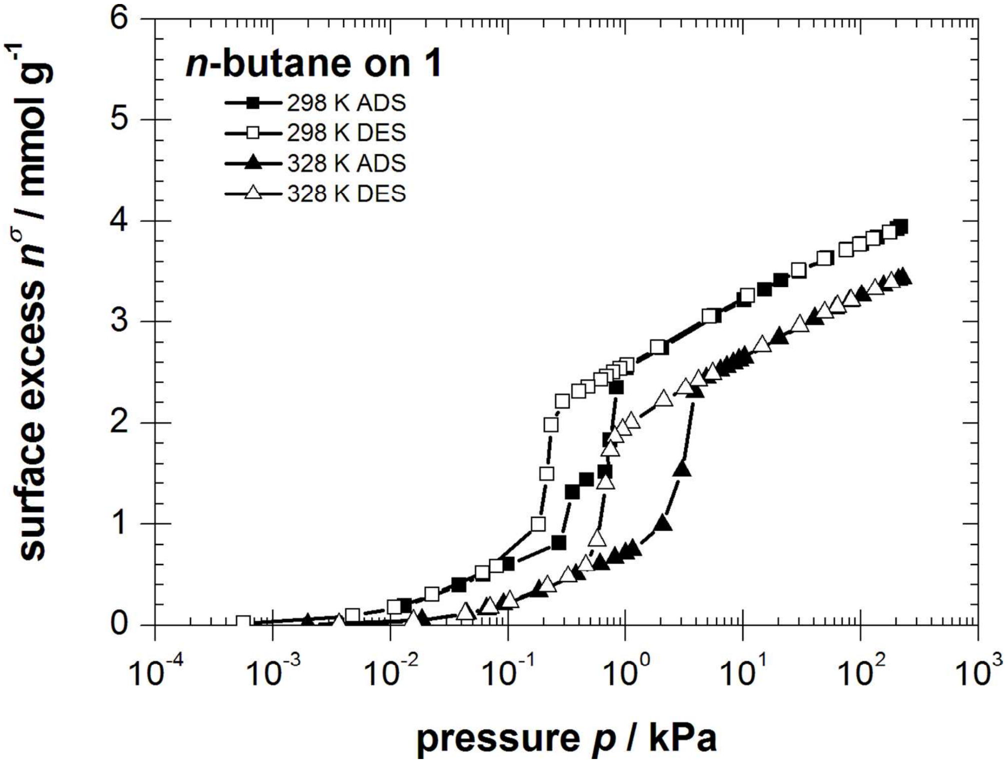
n-butane on 1
298 K ADS
298 K DES
328 K ADS
328 K DES
surface excess n^{σ} / mmol g^{-1}
0
1
2
3
4
5
6
10^{-4}
10^{-3}
10^{-2}
10^{-1}
10^{0}
10^{1}
10^{2}
10^{3}
pressure *p* / kPa

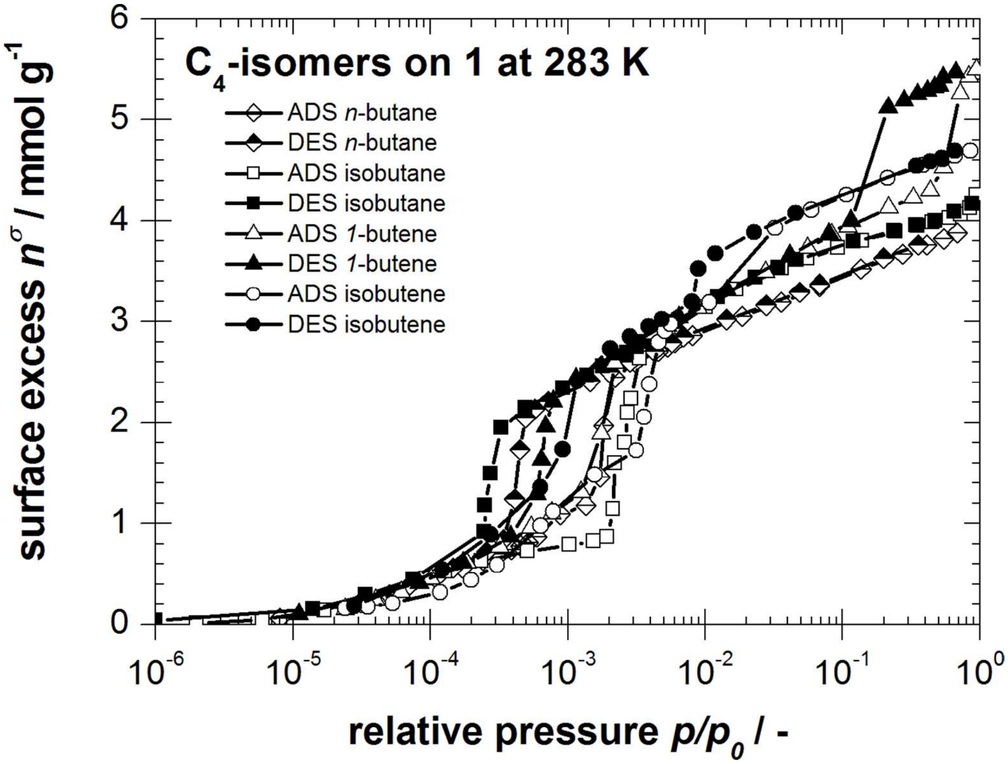
C4-isomers on 1 at 283 K
ADS n-butane
DES n-butane
ADS isobutane
DES isobutane
ADS 1-butene
DES 1-butene
ADS isobutene
DES isobutene
surface excess nσ / mmol g-1
relative pressure p/p0 / -
0
1
2
3
4
5
6
10-6
10-5
10-4
10-3
10-2
10-1
100

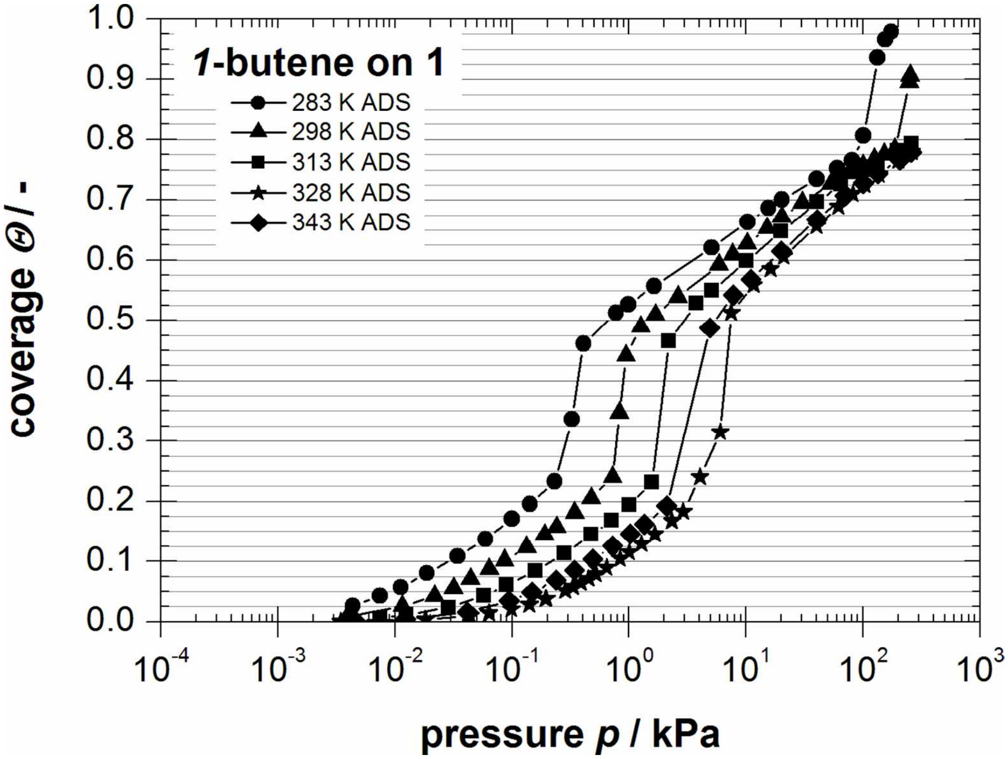

240x180mm (150 x 150 DPI)

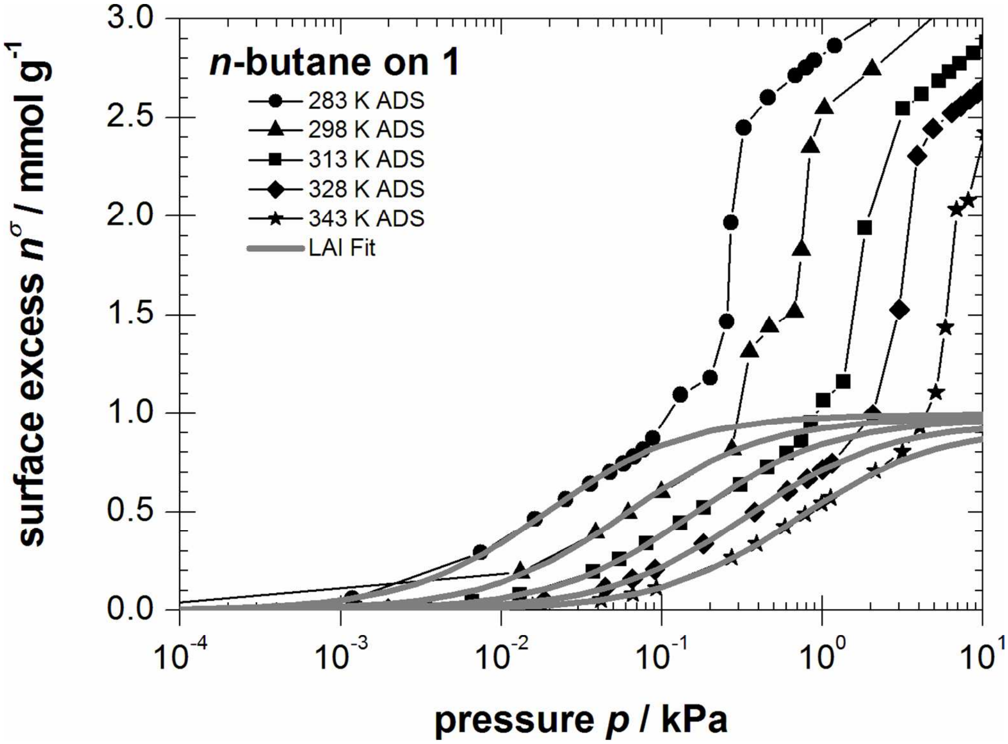

245x180mm (150 x 150 DPI)

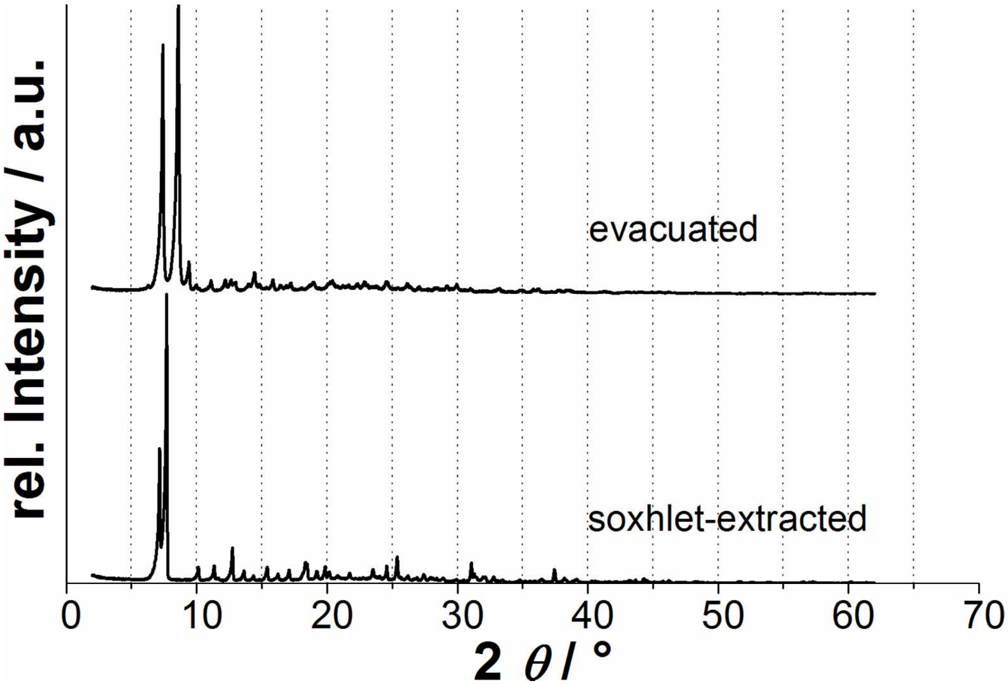

282x191mm (150 x 150 DPI)

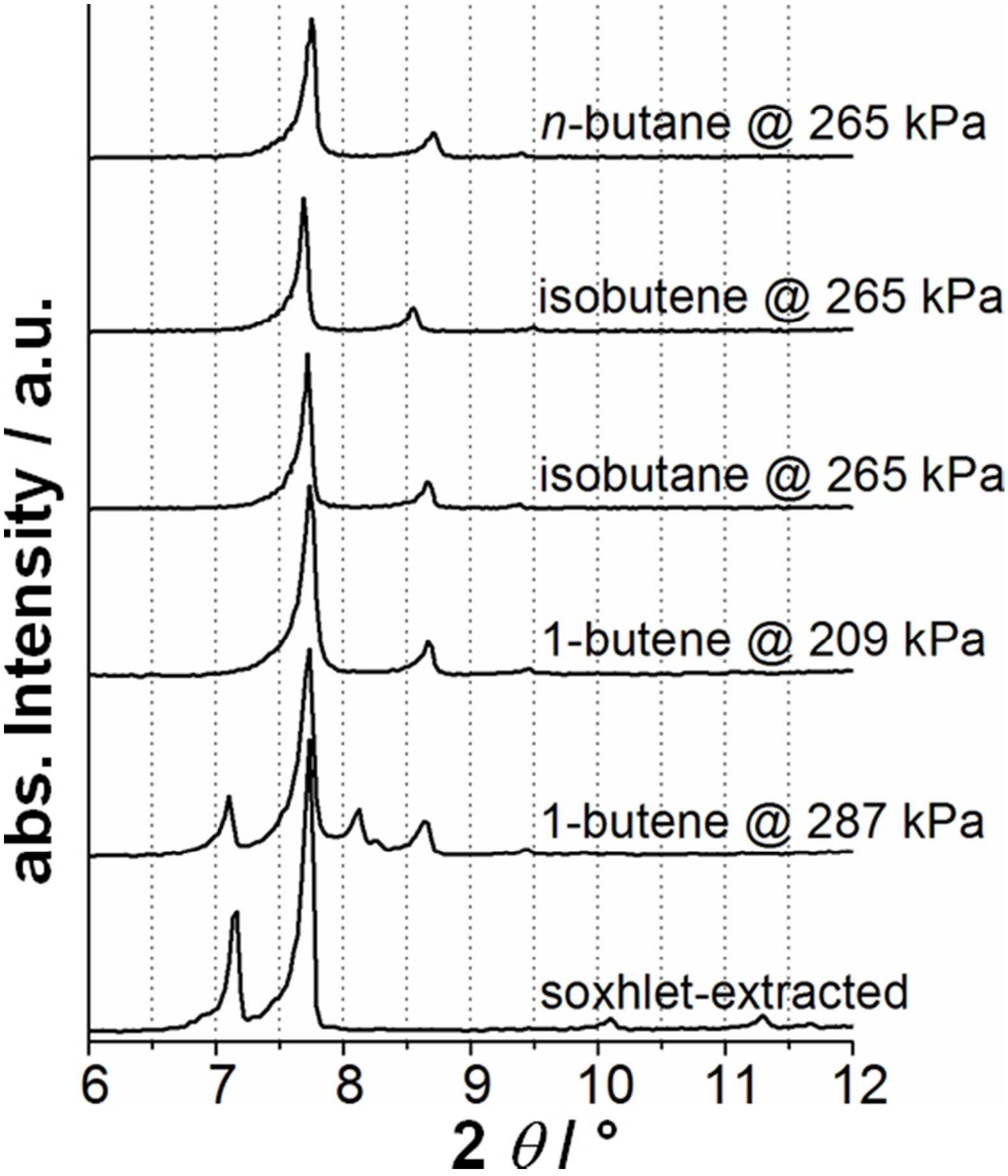
n-butane @ 265 kPa
isobutene @ 265 kPa
isobutane @ 265 kPa
1-butene @ 209 kPa
1-butene @ 287 kPa
soxhlet-extracted
abs. Intensity / a.u.
6
7
8
9
10
11
12
2 θ / °